PTEP

Prog. Theor. Exp. Phys. **2019**, 123I01 (30 pages)
DOI: 10.1093/ptep/ptz110

Thermodynamics of a generalized graphene-motivated (2 + 1)D Gross–Neveu model beyond the mean field within the Beth–Uhlenbeck approach

Dietmar Ebert[1,*] and David Blaschke[2,3,4,*]

[1]*Institut für Physik, Humboldt Universität zu Berlin, Newtonstraße 15, 12489 Berlin, Germany*
[2]*Instytut Fizyki Teoretycznej, Uniwersytet Wrocławski, pl. M. Borna 9, 50-204 Wrocław, Poland*
[3]*Laboratory of Theoretical Physics, Joint Institute for Nuclear Research, Joliot-Curie str. 6, 141980 Dubna, Russia*
[4]*Peoples' Friendship University of Russia (RUDN University), 6 Miklukho-Maklaya St, Moscow, 117198, Russia*
[*]E-mail: debert@physik.hu-berlin.de, david.blaschke@uwr.edu.pl

Received March 31, 2019; Revised July 30, 2019; Accepted August 29, 2019; Published December 3, 2019

We investigate the thermodynamics at finite density of a generalized (2 + 1)D Gross–Neveu model of N fermion species with various types of four-fermion interactions. The motivation for considering such a generalized schematic model arises from taking the Fierz transformation of an effective Coulomb current–current interaction and certain symmetry-breaking interaction terms, as considered for graphene-type models in Ref. [29]. We then apply path-integral bosonization techniques, based on the large-N limit, to derive the thermodynamic potential. This includes the leading-order mean-field (saddle point) contribution as well as the next-order contribution of Gaussian fluctuations of exciton fields. The main focus of the paper is then the investigation of the thermodynamic properties of the resulting fermion–exciton plasma. In particular, we derive an extended Beth–Uhlenbeck form of the thermodynamic potential, and discuss the Levinson theorem and the decomposition of the phase of the exciton correlation into resonant and scattering parts.

Subject Index I10, I32, I45, I46, I92

1. Introduction

The application of field-theoretic models with local four-fermion interactions to the investigation of fermion mass generation by spontaneous breakdown (SB) of symmetries and related phase transitions has a long history going back to the famous BCS–Bogoliubov approach to superconductivity [1, 2]. Important relativistic generalizations of this approach to strong interactions considering the dynamical generation of nucleon or quark masses due to SB of a continuous chiral γ_5 symmetry are the Nambu–Jona-Lasinio (NJL) model [3–10] or, in the case of lower dimensions $D = (1+1), D = (2+1)$, the Gross–Neveu (GN_2, GN_3) model with a discrete or continuous chiral symmetry [11–22]. Generally, such models are also extremely interesting for the generation of collective bosonic bound states. A powerful tool for deriving corresponding effective low-energy theories of collective bound states (mesons) from relativistic four-fermion models like NJL quark models are nonperturbative path-integral techniques (for detailed applications and references see, e.g., Refs. [6–10]).

It is interesting to note that in lower-dimensional condensed-matter systems like polymers [23, 24] or graphene [25], the low-energy fermion excitation spectrum is effectively described by a

© The Author(s) 2019. Published by Oxford University Press on behalf of the Physical Society of Japan.
This is an Open Access article distributed under the terms of the Creative Commons Attribution License (http://creativecommons.org/licenses/by/4.0/), which permits unrestricted reuse, distribution, and reproduction in any medium, provided the original work is properly cited.

Downloaded from https://academic.oup.com/ptep/article-abstract/2019/12/123I01/5651197 by Joint Institute for Nuclear Research user on 09 December 2019

(quasi)relativistic Dirac equation rather than by a Schrödinger equation. Such a similarity with relativistic quantum field theory (QFT) was a strong motivation to apply corresponding path-integral bosonization techniques, developed for relativistic quark models [5–10,26–28], to a quasirelativistic planar ($D = 2 + 1$) system like graphene [29]. Since the present work will continue the latter kind of investigation, let us shortly recall some main ideas of that work. There, one starts with an instantaneous four-fermion interaction obtained by a contact approximation to an instantaneous Coulomb potential using the "brane-world" or "reduced QED scenario", proposed in Ref. [30]. Next, performing a Fierz transformation into fermion–antifermion (hole) $f\bar{f}$-channels yields four different types of four-fermion interactions. This then leads—by means of the Hubbard–Stratonovich trick—to four types of possible exciton bound-state fields $E = \{\sigma_i, \varphi_i\}$, $i = 1, 2$. As a result, the four-fermion interactions are now changed into Yukawa-type bilinear ($Ef\bar{f}$)-couplings. After this, the fermion path integral becomes Gaussian and can easily be carried out. The resulting Fermion determinant, rewritten as a "Tr ln" term, then determines the effective low-energy action of collective exciton fields. Note that for the application of a suitable $1/N$ expansion technique, it was particular useful to consider the "multilayer" case of $N = 2\widetilde{N}$ degenerate fermion species (flavors) of real spin $\uparrow$ and $\downarrow$, living on $\widetilde{N}$ hexagonal monolayers. Thus, fermions carry here a flavor index $a = (1, \ldots, N = 2\widetilde{N})$. It is particularly important that in the case of graphene, there exist two "valley" degrees of freedom (d.o.f.) of fermions (corresponding to two "Dirac points"), which combine with two sublattice ("pseudospin") d.o.f. to form reducible four-spinors of a (quasi)relativistic Dirac theory. This just allows one to introduce chiral 4×4 Dirac matrices γ_5, γ_4, to consider a new emergent "pseudospin-valley" chiral $SU(2)_{\rm pv}$ symmetry and to study both the dynamical generation of fermion masses by SB of chiral symmetry and the resulting mass spectrum of composite excitons.

The considered graphene-motivated GN_3 model of Ref. [29] also includes small symmetry-breaking contributions due to on-site repulsive lattice interactions (as well as possible phonon-mediated interactions). Since the corresponding approximation scheme does not allow a determination of the effective coupling constants from an underlying microscopic lattice theory, this generalized GN_3 model can evidently be only considered as a schematic one. Nevertheless, because of its very general structure, we find it interesting for possible applications and specializations.

It is worth mentioning that in distinction to NJL quark models of strong interactions, the fermions of the considered generalized graphene-motivated GN_3 model are not confined. Thus, in contrast to the forbidden, artifact quark decay of a pion, $\pi \to q\bar{q}$, a real decay of a pseudoscalar exciton $E \to f\bar{f}$ is possible.

Finally, let us add some remarks on the problem of renormalization. As is well known, the GN_2 model is renormalizable and even asymptotically free [11,12]. On the other hand, the GN_3 model is perturbatively non-renormalizable, but becomes renormalizable in the $1/N$ expansion [16,17]. Anyway, in the condensed-matter motivated effective GN_3 model as considered in Ref. [29], there is no real problem with renormalization. Indeed, there exists a natural finite momentum cutoff $\Lambda \sim 1/a$ with a being the lattice spacing. In graphene $a \approx 2.46$ Å and $\Lambda \sim 1/a \approx 5$ keV.

The main goal of the present work is to extend the investigations of the generalized GN_3 model of Ref. [29], performed at $T = 0$, and to study its thermodynamics at finite temperature and fermion density (chemical potential) beyond the mean-field approximation. This requires calculation in the large-N limit of the thermodynamic potential of the model including both the dominating contribution of the fermion loop and the relative order $\mathcal{O}(1/N)$ correction term of exciton fluctuations around mean fields. The necessary calculations can be performed either by the diagrammatic summation of Feynman diagrams, as done for $D = (3 + 1)$D NJL models of colored quarks [31,32], or

Downloaded from https://academic.oup.com/ptep/article-abstract/2019/12/123I01/5651197 by Joint Institute for Nuclear Research user on 09 December 2019

by powerful path-integral methods at finite T, μ [33], which might be further combined with $1/N$ expansion techniques as in Refs. [20–22]. In the following we prefer to use an analogous large-N path-integral approach for calculating the grand canonical partition function and the related thermodynamic potential at (relative) order $\mathcal{O}(1/N)$. Note that besides explicit symmetry breaking in coupling constants, we also allow for explicit breaking of chiral symmetry by a bare fermion mass term m_0. This avoids dangerous IR-divergences [20–22] and, most importantly, excludes the validity of the Mermin–Wagner–Coleman (MWC) no-go theorem [34,35]. As is well known, the latter forbids SB of a continuous symmetry for a $(2+1)$D system at finite temperature.

The paper is organized as follows. In Sect. 2 we shortly review the generalized, graphene-motivated GN_3 model of Ref. [29] to be further studied in this paper, including necessary definitions and motivations. Section 3 starts with the path-integral representation of the grand canonical partition function and provides via the Hubbard–Stratonovich trick and after fermion integration the effective bosonized action of four types of bound-state exciton fields $E = \{\sigma_i, \varphi_i\}, i = (1, 2)$. The path integral over exciton fields becomes trivial, when evaluated in the large-N (saddle point) approximation for constant "mean-field" values, and leads to the mean-field approximation of the thermodynamic potential in Sect. 3.1. The respective mean-field values $\bar{\sigma}_i, \bar{\varphi}_i$ are determined from the stationarity (gap) equations as given by the minima of the thermodynamic potential. In the corresponding subsubsections, we first consider the vacuum gap equations at $T = 0$, $\mu = 0$ and then later the gap equation at finite temperature and chemical potential. In Sect. 3.2 we calculate the contribution of exciton fluctuations to the thermodynamic potential at (relative) order $\mathcal{O}(1/N)$ in the Gaussian approximation. They are given by the corresponding determinantal terms of inverse exciton propagators. The required polarization functions, entering the exciton propagators, are determined by fermion loop diagrams and calculated by standard Matsubara summation techniques. In Sect. 4 we present general expressions and equations for the mass spectrum of exciton bound and resonant states. Particular attention is paid to the possible formation of light (would-be) Goldstone excitons. They are generally expected to dominate the thermodynamics of a fermion–exciton plasma at low temperature. On the other hand, fermions become light due to restoration of chiral symmetry at high T and are expected to dominate in that region.

Finally, Sect. 5 contains the derivation of the celebrated Beth–Uhlenbeck (BU) formulation for the thermodynamics of a strongly correlated fermion system (cf. Refs. [31,32,36,37]), which we apply for the fermion–exciton plasma considered here. Note that the first application of the BU formula for plasma physics using phase shifts for the two-body scattering problem of the Coulomb interaction was given by Ebeling [38]. A generalization of the BU approach for excitons in dense electron–hole plasmas was developed by Zimmermann and Stolz (see Ref. [39] and references therein) and taken over to the problem of bound-state formation in nuclear matter in Ref. [40]. In the present work we will restrict ourselves to the low-density limit. Using the pole approximation, we also quote the pressure of a gas of free excitons and consider a first departure beyond such an approximation based on a Breit–Wigner-type ansatz for the density of states. Moreover, similarly to Refs. [31,32,41,42], we indicate here the necessity of a decomposition of the scattering phase shift into resonant and scattering parts in order to fulfill the Levinson theorem. In Sect. 6 we summarize our main results and present the conclusions. Technical details like the algebra of Dirac matrices in $D = 3$, the explicit solution of the vacuum gap equations, and the calculation of the exciton polarization functions are relegated to the three appendices.

Downloaded from https://academic.oup.com/ptep/article-abstract/2019/12/123I01/5651197 by Joint Institute for Nuclear Research user on 09 December 2019

2. Generalized GN model: definitions and motivations

In the following we shall consider a planar system of N fermion species (flavors) described by a generalized, graphene-motivated $(2+1)$D Gross–Neveu (GN) type of model, analogous to that considered in Refs. [15,29].

Using Euclidean notations, the Lagrangian $\mathcal{L}_e$, $\mathcal{L}_e = -\mathcal{L}|_{t\to -i\tau}$, is given by a sum of two terms

$$\mathcal{L}_e = \mathcal{L}_0 + \mathcal{L}_{\rm int}, \tag{1}$$

where $\mathcal{L}_0$ is the free part including a (small) bare fermion mass m_0 supplemented by a chemical potential μ,

$$\mathcal{L}_0 = \bar\psi\left(\gamma_\mu\partial_\mu - \mu\gamma_3 + m_0\right)\psi, \tag{2}$$

and $\mathcal{L}_{\rm int}$ describes a generalized local four-fermion interaction with different coupling structures given by[1]

$$\mathcal{L}_{\rm int} = -\left\{\frac{G_1}{2N}\left(\bar\psi\psi\right)^2 + \frac{G_2}{2N}\left(\bar\psi\gamma_{45}\psi\right)^2 + \frac{H_1}{2N}\left(\bar\psi i\gamma_5\psi\right)^2 + \frac{H_2}{2N}\left(\bar\psi i\gamma_4\psi\right)^2\right\}. \tag{3}$$

Note that the fermion field $\psi(x)$ in the Lagrangian $\mathcal{L}_e$ transforms as a fundamental multiplet of the flavor group $U(N)$, i.e., $\psi(x) = \{\psi_a(x)\}$ with $a = 1,\ldots,N$. Moreover, each component $\psi_a(x)$ of this multiplet is taken to be a four-component Dirac spinor that transforms according to a reducible 4D representation of the rotation group $SO(3)$. The reason for this choice is our interest in chiral symmetry and its possible dynamical breakdown in planar systems like graphene, which require the existence of a chiral γ_5 matrix. As is well known, such a matrix can only be obtained in $(2+1)$ dimensions by using a reducible 4×4 representation of Dirac matrices [16,17,43]. Note further that G_i, H_i are general coupling constants, and γ_μ $(\mu = 1,\ldots,3)$, γ_4, γ_5, γ_{45} are Dirac matrices discussed in detail in Appendix A.

Since the main purpose of this paper is to study the planar many-body system of fermions and composite excitons at finite temperature and fermion density (finite μ), we find it convenient to use from the very beginning Euclidean notations for the Lagrangian, coordinates $x_\mu = (x_1, x_2, x_3 = \tau) = (\vec{x}, x_3)$ $(it = \tau)$ and γ matrices. Finally, let us remark that spinor and $U(N)$-group indices are not given explicitly and summation over them is implied everywhere; moreover, the index at $\mathcal{L}_e$ will now be omitted.

Note that the kinetic part of the free Lagrangian $\mathcal{L}_0$ is invariant under discrete chiral transformations

$$\gamma_5 : \psi \to \gamma_5\psi, \quad \bar\psi \to -\bar\psi\gamma_5, \tag{4}$$

$$\gamma_4 : \psi \to \gamma_4\psi, \quad \bar\psi \to -\bar\psi\gamma_4, \tag{5}$$

and under the discrete operations of spatial inversion $\mathcal{P}$, time reversal $\mathcal{T}$, and charge conjugation $\mathcal{C}$. Recall that in the reducible (4D) representation of the Clifford algebra, the definition of the discrete transformations $\mathcal{P}, \mathcal{T}, \mathcal{C}$ is not unique. Bearing in mind the condensed-matter roots of the graphene-motivated GN_3 model considered above, the discrete symmetry operations will suitably be taken here

[1] In this paper we shall use natural units $\hbar = c = k_{\rm B} = 1$, where $k_{\rm B}$ is the Boltzmann constant. Comparing with the particular case of graphene, the Fermi velocity $v_{\rm F}$ appearing in the effective Lagrangian is then also dimensionless and might be considered here, for notational simplicity, as $v_{\rm F} = 1$. The realistic value of $v_{\rm F}$ ($v_{\rm F} \approx 1/300$) can be easily re-established by dimensional considerations (see, e.g., Ref. [29]). Note that for pure graphene $m_0 = 0$, and fields of fermions f are denoted by ψ.

Downloaded from https://academic.oup.com/ptep/article-abstract/2019/12/123I01/5651197 by Joint Institute for Nuclear Research user on 09 December 2019

Table 1. Transformation properties of various fermion bilinears $\bar{\psi}\Gamma_A\psi$, $\Gamma_A = (\Gamma_i, \widetilde{\Gamma}_i)$ (compare Eq. (20) below), and the current $\bar{\psi}\gamma_\mu\psi$ under the discrete transformations described in the text. In the case of spatial reflections the transformed bilinears depend on reversed coordinates, and we have $\widetilde{\gamma_\mu} = (-\gamma_1, -\gamma_2, \gamma_3)$. Note that in Euclidean space, the spatial components of the current do not change under $\mathcal{T}$.

$\bar{\psi}\Gamma_A\psi$	$\bar{\psi}\psi$	$\bar{\psi}\gamma_{45}\psi$	$\bar{\psi}i\gamma_5\psi$	$\bar{\psi}i\gamma_4\psi$	$\bar{\psi}\gamma_\mu\psi$
$\mathcal{P}$	1	1	−1	−1	$\bar{\psi}\widetilde{\gamma_\mu}\psi$
$\mathcal{T}$	1	−1	1	1	$\bar{\psi}\gamma_\mu\psi$
$\mathcal{C}$	1	1	−1	1	$-\bar{\psi}\gamma_\mu\psi$
γ_5	−1	1	−1	1	$\bar{\psi}\gamma_\mu\psi$
γ_4	−1	1	1	−1	$\bar{\psi}\gamma_\mu\psi$

in such a way that they are consistent with the underlying tight-binding model on the honeycomb lattice (see Ref. [44]).

By slightly modifying the corresponding definitions of Ref. [44] when using the imaginary-time formalism of equilibrium thermodynamics, Euclidean notations for Dirac matrices, and Grassmann fields for fermions as required in path integrals (for explanations and details, see Appendix A.3), one has

$$\mathcal{P}: \quad \psi(\vec{x},x_3) \to \gamma_3\psi(-\vec{x},x_3),\ \bar{\psi}(\vec{x},x_3) \to \psi^\dagger(-\vec{x},x_3), \tag{6}$$

$$\mathcal{T}: \quad \psi(\vec{x},x_3) \to (i\sigma_2)i\gamma_1\gamma_5\psi(\vec{x},x_3),\ \bar{\psi}(\vec{x},x_3) \to -\bar{\psi}(\vec{x},x_3)i\gamma_1\gamma_5(i\sigma_2), \tag{7}$$

$$\mathcal{C}: \quad \psi(\vec{x},x_3) \to i\gamma_1\bar{\psi}^t(\vec{x},x_3),\ \bar{\psi}(\vec{x},x_3) \to (-i\gamma_1\psi(\vec{x},x_3))^t. \tag{8}$$

Here the spin matrix σ_2 in $\mathcal{T}$ acts on the indices of physical spin included in the combined flavor index a suppressed here, and the superscript t denotes transposition. (Note that in Euclidean space $\mathcal{T}$ does not change the sign of Euclidean time x_3.)

The respective transformation properties of various fermion bilinears under discrete operations $\mathcal{P}, \mathcal{T}, \mathcal{C}$ of spatial inversion, time reversal, charge conjugation, and under chiral transformations with γ_5, γ_4 are shown in Table 1. It then follows that $\mathcal{L}_0$ is invariant under $\mathcal{P}$, $\mathcal{T}$, and $\mathcal{C}$ (with the restriction $\mu \to -\mu$ for $\mathcal{C}$). Moreover, since $\mathcal{L}_{\rm int}$ depends quadratically on fermion bilinears, it follows from Table 1 that the total Lagrangian $\mathcal{L}$ is also invariant.

Let us next also consider continuous chiral transformations γ_5 and γ_4:

$$U_{\gamma_5}(1): \psi \to \exp(i\alpha\gamma_5)\psi,\ \ \bar{\psi} \to \bar{\psi}\exp(i\alpha\gamma_5), \tag{9}$$

$$U_{\gamma_4}(1): \psi \to \exp(i\tilde{\alpha}\gamma_4)\psi,\ \ \bar{\psi} \to \bar{\psi}\exp(i\tilde{\alpha}\gamma_4). \tag{10}$$

Taking certain symmetry restrictions like $G_1 = H_1$ (G_2, H_2 arbitrary) or $G_1 = H_2$ (G_2, H_1 arbitrary), the Lagrangian $\mathcal{L}$ of Eq. (1) is even invariant under continuous chiral γ_5 and γ_4 transformations.

It is worth remarking that in the case of a continuous chiral transformation $\mathrm{U}_{\gamma_5}(1)$ fermion bilinears transform as follows:

$$\begin{aligned}
(\bar{\psi}\psi) &\to (\bar{\psi}\psi)\cos(2\alpha) + (\bar{\psi}i\gamma_5\psi)\sin(2\alpha),\\
(\bar{\psi}i\gamma_5\psi) &\to -(\bar{\psi}\psi)\sin(2\alpha) + (\bar{\psi}i\gamma_5\psi)\cos(2\alpha),\\
(\bar{\psi}i\gamma_4\psi) &\to (\bar{\psi}i\gamma_4\psi),\\
(\bar{\psi}\gamma_{45}\psi) &\to (\bar{\psi}\gamma_{45}\psi).
\end{aligned} \tag{11}$$

Downloaded from https://academic.oup.com/ptep/article-abstract/2019/12/123I01/5651197 by Joint Institute for Nuclear Research user on 09 December 2019

Analogous relations hold for continuous chiral γ_4 transformations.

Let us remark that particular cases of the interaction part (3), e.g., a discrete GN model ($G_2 = H_{1,2} = 0$) (see, e.g., Refs. [11–14,20–22,43]) or a chiral Nambu–Jona-Lasinio type of model ($G_1 = H_1,\ G_2 = H_2 = 0$) (see, e.g., Refs. [16,17,20–22] and references therein), have already been studied earlier in the literature. Our motivation for studying the generalized GN type of model (3) comes from the investigation of effective Coulomb interactions in hexagonal, graphene-like lattice sheets [29],

$$\Delta\mathcal{L}_{\rm int}^{\rm Coul} = \frac{G^C}{2}\left(\bar\psi\gamma_3\psi\right)^2, \tag{12}$$

possibly supplemented by a small symmetry-breaking on-side repulsive interaction term and analogous terms from phonon-mediated interactions, which in summary are given by

$$\Delta\mathcal{L}_{\rm int}^{\rm sb} = -\frac{\widetilde{G}}{2}\left(\bar\psi\psi\right)^2,\ \widetilde{G} < 0. \tag{13}$$

It is worth remarking that in the chiral limit ($m_0 = 0$) the free Lagrangian (2) and the Coulomb-interaction part (12) of graphene are invariant under the emergent "pseudospin-valley" symmetry group $SU(2)_{\rm pv}$ with generators $t_1 = \frac{1}{2}\gamma_4$, $t_2 = \frac{1}{2}\gamma_5$, $t_3 = \frac{1}{2}\gamma_{45}$ (see Eqs. (A.5), (A.6) in Appendix A). Note that we have introduced the flavor group $U(N)$ for later use in a $1/N$ expansion. In the corresponding "multilayer" case of graphene (see Ref. [29]), one has $N = 2\widetilde{N}$ degenerate fermion species (flavors) of real spin $\uparrow$ and $\downarrow$ living on $\widetilde{N}$ hexagonal monolayers. In addition to the emergent $U(2)_{\rm pv} = U(1)_{\rm pv} \otimes SU(2)_{\rm pv}$ invariance and the flavor $U(N)$ invariance, there also arises invariance under the larger group $U(2N)$.[2]

Next, by performing a Fierz transformation into bound-state interaction channels for composite exciton fields $\Phi_A \sim \bar\psi\Gamma_A\psi$, $\Gamma_A = \{I, \gamma_{45}; i\gamma_5, i\gamma_4\}$, and discarding, for simplicity, vector/axial-vector type interactions, we obtain from Eqs. (12), (13) the expression $\mathcal{L}_{\rm int} = \Delta\mathcal{L}_{\rm int}^{\rm Coul} + \Delta\mathcal{L}_{\rm int}^{\rm sb}$ [29],

$$\mathcal{L}_{\rm int} = -\left\{\frac{G_1'}{2N}\left[\left(\bar\psi\psi\right)^2 + \left(\bar\psi\gamma_{45}\psi\right)^2\right] + \frac{G_2'}{2N}\left[\left(\bar\psi i\gamma_5\psi\right)^2 + \left(\bar\psi i\gamma_4\psi\right)^2\right]\right\}, \tag{14}$$

where

$$G_1' = \frac{1}{4}\left(G^C - \widetilde{G}\right),\ G_2' = \frac{1}{4}\left(G^C + \widetilde{G}\right). \tag{15}$$

Comparing this with the general expression (3), one has $G_1 = G_2 = G_1', H_1 = H_2 = G_2'$. Neglecting further the symmetry-breaking term (13), i.e., setting $\widetilde{G} = 0$, one gets the symmetric case $G_1' = G_2'$, i.e., $G_i = H_i$ $(i = 1, 2)$, reflecting the $SU(2)$ symmetry of the electromagnetic Coulomb interaction.

Clearly, the approximation scheme employed does not allow a determination of the effective coupling constants $G_{1,2}'$ arising from an underlying microscopic lattice theory, eventually including lattice vibrations. Thus, the above four-fermion interaction (14) can only be considered as a schematic one. In the following we shall therefore consider its most general form (3) and specify,

[2] Note that the symmetry-breaking term (13) breaks the larger group $U(2N)$, $U(2N) \to U(N)_{t_0} \otimes U(N)_{t_3}$. Here the Lie algebra of the groups $U(N)_{t_0,t_3}$ is given by the direct product of respective generators $t_0 = \frac{1}{2}I$, t_3 of $U(2)_{\rm pv}$ with the generators of $U(N)$ [29].

Downloaded from https://academic.oup.com/ptep/article-abstract/2019/12/123I01/5651197 by Joint Institute for Nuclear Research user on 09 December 2019

for illustration, more symmetric cases, if necessary. Before concluding this subsection, let us add a remark on Lorentz invariance. Clearly, due to the suppression of spatial components of currents and related retardation effects in the considered four-fermion interaction in graphene, the chiral invariant Coulomb expression (12) and its Fierz transformation is not Lorentz-invariant. However, this does not matter here, since (again discarding the resulting vector/axial-vector interaction terms), the Fierz transformation of a corresponding Lorentz-invariant Thirring-like vector interaction reproduces, up to a factor of 3, the structure (14) ($\widetilde{G} = 0$) (see, e.g., Eqs. (A.8), (A.9) of Appendix A in Ref. [29]).

3. Grand canonical partition function

The thermodynamics of the considered generalized GN model at finite temperature T and chemical potential μ is most conveniently described by the grand canonical partition function

$$\mathcal{Z}(T,\mu) = \mathrm{Tr}\, e^{-\beta(H-\mu Q)}. \tag{16}$$

Here H is the Hamiltonian of the system, $Q = \bar{\psi}\gamma_3\psi$ is the charge operator, and $\beta = 1/T$ with T being the temperature. It is well known that $\mathcal{Z}(T,\mu)$ can be expressed as a path integral,

$$\mathcal{Z}(T,\mu) = \int \mathcal{D}\bar{\psi}\mathcal{D}\psi \exp\left[-\int d^3x\mathcal{L}\right], \tag{17}$$

where $\mathcal{L}$ is the model Lagrangian (1)–(3), and

$$\int d^3x = \int_A d^2\vec{x}\int_0^\beta d\tau \tag{18}$$

denotes integration over the imaginary time ($\tau = it$) interval $\tau \in [0, \beta = 1/T]$ and the plane with area $A = l^2$. Note that the fermionic Grassmann fields in Eq. (17) satisfy *antiperiodic* boundary conditions $\psi(\vec{x},0) = -\psi(\vec{x},\beta)$.

As usual, performing the fermionic path integral (17) with four-fermion interactions requires a Hubbard–Stratonovich transformation by introducing composite scalar (σ_1, σ_2) and pseudoscalar (φ_1, φ_2) exciton fields. The transformed Lagrangian of the generalized GN model then takes the form

$$\begin{aligned}\mathcal{L}\left[\bar{\psi},\psi,\sigma_i,\varphi_i\right] = N\sum_{k=1}^{2}\left[\frac{\sigma_k^2}{2G_k}+\frac{\varphi_k^2}{2H_k}\right]\\ +\bar{\psi}\left[\gamma\partial-\mu\gamma_3+(m_0+\sigma_1)+\sigma_2\gamma_{45}+\varphi_1 i\gamma_5+\varphi_2 i\gamma_4\right]\psi.\end{aligned} \tag{19}$$

Obviously, by inserting the field equations for exciton fields ($i = 1,2$)

$$\begin{aligned}\sigma_i &= -\frac{G_i}{N}\bar{\psi}\Gamma_i\psi\ ,\ \Gamma_i = \{I,\gamma_{45}\},\\ \varphi_i &= -\frac{H_i}{N}\bar{\psi}\widetilde{\Gamma}_i\psi\ ,\ \widetilde{\Gamma}_i = \{i\gamma_5, i\gamma_4\}\end{aligned} \tag{20}$$

back into expression (19) reproduces the original form of the Lagrangian $\mathcal{L}$ in Eq. (1)[3]. Note that for a constant field $\sigma_1 \equiv \langle\sigma_1\rangle$, $m = m_0 + \langle\sigma_1\rangle$ can obviously be interpreted as a dynamical fermion mass.

[3] Note that the factor 1/4 in the Gaussian term of exciton fields, appearing in Eq. (40) of Ref. [29], is incorrect and has to be replaced by 1/2, as shown in Eq. (19) of this text. Correspondingly, Eq. (20) does not contain a factor 2.

Downloaded from https://academic.oup.com/ptep/article-abstract/2019/12/123I01/5651197 by Joint Institute for Nuclear Research user on 09 December 2019

It is worth remarking that taking the grand canonical expectation values (condensates $\langle\cdots\rangle$) of both sides of Eq. (20) relates condensates of exciton fields ($\langle\sigma_i\rangle$, $\langle\phi_i\rangle$) to condensates of corresponding fermion bilinears $\langle\bar\psi\Gamma_A\psi\rangle$, $\Gamma_A = \left(\Gamma_i, \widetilde{\Gamma}_i\right)$.[4]

Using Eqs. (17), (19) and performing a field shift $\sigma_1 \to \sigma_1 - m_0$, the grand canonical partition function now takes the form ($\kappa = m_0/G_1$)

$$\mathcal{Z}(T,\mu) = \int \prod_{i=1}^{2} \mathcal{D}\sigma_i \mathcal{D}\varphi_i \exp\left[-\int d^3xN \sum_{k=1}^{2}\left(\frac{\sigma_k^2}{2G_k} + \frac{\varphi_k^2}{2H_k} - \delta_{k1}\kappa\sigma_1\right)\right] \times \int \mathcal{D}\bar\psi\mathcal{D}\psi \exp\left[-\int d^3x \int d^3y\, \bar\psi(x)\hat{S}^{-1}(x,y)\psi(y)\right], \tag{21}$$

where bosonic exciton fields must satisfy *periodic* boundary conditions, $\sigma_k(\vec{x},0) = \sigma_k(\vec{x},\beta)$, $\varphi_k(\vec{x},0) = \varphi_k(\vec{x},\beta)$. Moreover, the inverse fermion propagator $\hat{S}^{-1}(x,y)$ in Eq. (21) is given by

$$\begin{aligned}\hat{S}^{-1}(x,y) &= (\gamma\partial - \mu\gamma_3 + \sigma_1(x) + \sigma_2(x)\gamma_{45} + \varphi_1(x)i\gamma_5 + \varphi_2(x)i\gamma_4)\,\delta^{(3)}(x-y)\mathbf{1} \\ &= S^{-1}(x,y)\mathbf{1}.\end{aligned} \tag{22}$$

The resulting Gaussian path integral over fermion fields can easily be performed and leads to a fermion determinant

$$\left[\det S^{-1}\right]^N = \exp\left[N\mathrm{Tr}\ln S^{-1}\right], \tag{23}$$

where the Tr symbol means the functional trace of an operator both in Euclidean coordinates and Dirac space, respectively. The grand canonical partition function is now expressed in terms of (bosonic) exciton fields alone and reads

$$\mathcal{Z}(T,\mu) = \int \prod_{i=1}^{2} \mathcal{D}\sigma_i \mathcal{D}\varphi_i \exp\left\{-N\left[\int d^3x \sum_{k=1}^{2}\left(\frac{\sigma_k^2}{2G_k} + \frac{\varphi_k^2}{2H_k} - \delta_{k1}\kappa\sigma_1\right) - \mathrm{Tr}\ln S^{-1}\right]\right\}. \tag{24}$$

3.1. Mean-field approximation

As a first step, we now calculate the determinantal term $-\mathrm{Tr}\ln S^{-1}$ for *constant* exciton fields, as considered in the large-N (mean-field, "mf") saddle point approximation of the path integral. The calculations are conveniently done by Fourier transforming the fermion fields in the respective path integral (see, e.g., Refs. [45]):

$$\psi_\alpha(\vec{x},\tau) = \frac{1}{l}\sum_n \sum_{\vec{p}} e^{-i(\omega_n\tau + \vec{p}\cdot\vec{x})}\widetilde{\psi}_{\alpha n}(\vec{p}), \tag{25}$$

where the index α refers here to the (reducible) four-component Dirac spinor, $\omega_n = (2n+1)\pi/\beta$, $n = 0, \pm1, \pm2, \ldots$ are fermionic Matsubara frequencies, and $\widetilde{\psi}_{\alpha n}(\vec{p})$ is dimensionless. Obviously, in the mf (large-N saddle point) approximation the path integral (24), evaluated at constant mf

[4] Recall that $\langle\bar\psi\Gamma_A\psi\rangle := \mathrm{Tr}\left\{\left(\bar\psi\Gamma_A\psi\right)\exp\left[-\beta(H-\mu Q)\right]\right\}/\mathcal{Z} = \int\mathcal{D}\bar\psi\,\mathcal{D}\psi\left(\bar\psi\Gamma_A\psi\right)\exp\left[-\int d^3x\mathcal{L}\right]/\mathcal{Z}$.

Downloaded from https://academic.oup.com/ptep/article-abstract/2019/12/123I01/5651197 by Joint Institute for Nuclear Research user on 09 December 2019

values $(\sigma_k, \varphi_k)_{\rm mf}$, becomes trivial and the grand canonical partition function factorizes. The relevant thermodynamic quantity, closely related to $\mathcal{Z}$, is the thermodynamic potential per area $A = l^2$:

$$\Omega(T,\mu) = -\frac{1}{\beta l^2} \ln \mathcal{Z}(T,\mu). \tag{26}$$

Its mean-field expression can be separated into an excitonic condensate part and a fermionic contribution, respectively,

$$\Omega_{\rm mf} = \Omega_{\rm cond} + \Omega_{\rm f}, \tag{27}$$

where

$$\Omega_{\rm cond} = N \sum_{k=1}^{2} \left[\left(\frac{\sigma_k^2}{2G_k} + \frac{\varphi_k^2}{2H_k} - \delta_{k1}\kappa\sigma_1 \right)_{\rm mf} \right], \tag{28}$$

$$\Omega_{\rm f} = -\frac{1}{\beta l^2} N {\rm Tr} \ln \left(\beta S_{\rm mf}^{-1} \right), \tag{29}$$

and

$$S_{\rm mf}^{-1}(\vec{p},\omega_n) = (-i\gamma_3(\omega_n - i\mu) - i\vec{\gamma}\cdot\vec{p} + \sigma_1 + \sigma_2\gamma_{45} + \varphi_1 i\gamma_5 + \varphi_2 i\gamma_4)_{\rm mf} \tag{30}$$

is the inverse mean-field fermion propagator in $(\vec{p},\omega_n)$ space. Obviously, $\Omega_{\rm mf} = \mathcal{O}(N)$ for large N. Note that the exciton mean-field values $(\sigma_k,\varphi_k)_{\rm mf} \equiv (\bar{\sigma}_k(T,\mu), \bar{\varphi}_k(T,\mu))$ at finite temperature T and chemical potential μ are obtained as minima (stationary points) of the thermodynamic potential per flavor species:

$$0 = \frac{1}{N}\frac{\partial\Omega}{\partial\sigma_k}\bigg|_{\rm mf} = \left(\frac{\sigma_k}{G_k} - \kappa\delta_{k1} - \frac{1}{\beta l^2} {\rm Tr} S \frac{\partial S^{-1}}{\partial\sigma_k} \right)_{\rm mf}, \tag{31}$$

$$0 = \frac{1}{N}\frac{\partial\Omega}{\partial\varphi_k}\bigg|_{\rm mf} = \left(\frac{\varphi_k}{H_k} - \frac{1}{\beta l^2} {\rm Tr} S \frac{\partial S^{-1}}{\partial\varphi_k} \right)_{\rm mf}, \tag{32}$$

where $\frac{1}{N}\frac{\partial^2\Omega}{\partial\sigma_k^2}\Big|_{\rm mf} > 0$, $\frac{1}{N}\frac{\partial^2\Omega}{\partial\varphi_k^2}\Big|_{\rm mf} > 0$ and

$$\frac{\partial S^{-1}}{\partial\sigma_k}\bigg|_{\rm mf} = \Gamma_k\,, \quad k = 1,2, \tag{33}$$

$$\frac{\partial S^{-1}}{\partial\varphi_k}\bigg|_{\rm mf} = \widetilde{\Gamma}_k\,, \quad k = 1,2, \tag{34}$$

with Γ_k, $\widetilde{\Gamma}_k$ being defined in Eq. (20). From Eq. (20) it follows that the mean-field values (condensates) $(\bar{\sigma}_k,\bar{\varphi}_k) \equiv (\langle\sigma_k\rangle, \langle\varphi_k\rangle)$ correspond to the fermion condensates $\langle\bar{\psi}\Gamma_k\psi\rangle$, $\langle\bar{\psi}\widetilde{\Gamma}_k\psi\rangle$.

Let us next consider the fermion contribution (29). Performing the functional trace Tr, which is now defined as a sum over Matsubara frequencies ω_n, two-momenta $\vec{p}$ and including the trace tr over Dirac indices, i.e.,

$${\rm Tr} = \sum_{n,\vec{p}} {\rm tr} = l^2 \sum_n \int \frac{d^2p}{(2\pi)^2} {\rm tr}, \tag{35}$$

Downloaded from https://academic.oup.com/ptep/article-abstract/2019/12/123I01/5651197 by Joint Institute for Nuclear Research user on 09 December 2019

we obtain

$$\Omega_{\rm f} = -\frac{N}{\beta}\sum_n \int \frac{d^2p}{(2\pi)^2} {\rm tr}\ln\left(\beta S_{\rm mf}^{-1}\right) = -\frac{N}{\beta}\sum_n \int \frac{d^2p}{(2\pi)^2}\sum_i \ln\left(\beta\varepsilon_i\right). \tag{36}$$

Here ε_i are the four eigenvalues of the 4×4 matrix $S_{\rm mf}^{-1}$, which are given by (see Refs. [15,29])

$$\varepsilon_{1,2,3,4} = \bar{\sigma}_1 \pm \sqrt{\left(\bar{\sigma}_2 \pm \sqrt{-(\omega_n - i\mu)^2 - \vec{p}^2}\right)^2 - \bar{\varphi}_1^2 - \bar{\varphi}_2^2}. \tag{37}$$

Then, $\Omega_{\rm f}$ takes the form

$$\Omega_{\rm f} = -\frac{N}{\beta}\sum_{k=1}^{2}\int \frac{d^2p}{(2\pi)^2}\sum_n \ln\left\{\beta^2\left[(\omega_n - i\mu)^2 + E_p^{(k)^2}\right]\right\}, \tag{38}$$

where

$$E_p^{(k)} = \sqrt{\vec{p}^2 + M_k^2} \tag{39}$$

and

$$M_{1,2} = \bar{\sigma}_2 \pm \bar{\varrho}\ ,\ \bar{\varrho} = \sqrt{\bar{\sigma}_1^2 + \bar{\varphi}_1^2 + \bar{\varphi}_2^2} \tag{40}$$

are energies or masses associated with two (correspondingly projected) quasiparticle fields, $\psi_{1,2} = \frac{1}{2}\left(1 \pm \gamma_{45}\right)\psi$.

Using standard techniques for performing the Matsubara summation of the logarithmic terms in Eq. (38) (see, e.g., Ref. [45]), we arrive at the final expression:

$$\Omega_{\rm f} = -N\sum_{k=1}^{2}\int \frac{d^2p}{(2\pi)^2}\left[E_p^{(k)} + \frac{1}{\beta}\ln\left(1 + e^{-\beta(E_p^{(k)} - \mu)}\right) + \frac{1}{\beta}\ln\left(1 + e^{-\beta(E_p^{(k)} + \mu)}\right)\right]. \tag{41}$$

3.1.1. Vacuum gap equations

Obviously, the first term in the square bracket of Eq. (41) is just the vacuum contribution at $T = 0$, $\mu = 0$, whereas the other terms describe the contributions of a free gas of two types of N quasiparticles (antiquasiparticles) of masses M_1 and M_2 at T and μ. Note that the vacuum contribution contains a UV-divergent momentum integral that will be regularized by a cutoff Λ, using polar coordinates for momenta, i.e., $|\vec{p}| < \Lambda$. The regularized vacuum contribution to the thermodynamic potential $\Omega_{\rm vac}\ (T = 0, \mu = 0)$,

$$\Omega_{\rm vac}^{\rm reg}(0,0) = N\sum_{k=1}^{2}\left[\left(\frac{\bar{\sigma}_k^2}{2G_k} + \frac{\bar{\varphi}_k^2}{2H_k} - \delta_{k1}\kappa\bar{\sigma}_1\right) - \int_\Lambda \frac{d^2p}{(2\pi)^2}E_p^{(k)}\right], \tag{42}$$

then takes the form (cf. Ref. [15,29])

$$\Omega_{\rm vac}^{\rm reg}(0,0) = N\sum_{k=1}^{2}\left[\frac{1}{2}\left(G_k^{-1} - \frac{\Lambda}{\pi}\right)\bar{\sigma}_k^2 + \frac{1}{2}\left(H_k^{-1} - \frac{\Lambda}{\pi}\right)\bar{\varphi}_k^2 - \delta_{k1}\kappa\bar{\sigma}_1 + \frac{|M_k|^3}{6\pi}\right], \tag{43}$$

where, supposing $M_k \ll \Lambda$, a term $|M_k|^3\mathcal{O}\left(\frac{M_k}{\Lambda}\right)$ was omitted.

Downloaded from https://academic.oup.com/ptep/article-abstract/2019/12/123I01/5651197 by Joint Institute for Nuclear Research user on 09 December 2019

It is convenient to eliminate the cutoff parameter Λ in Eq. (43) by introducing renormalized coupling constants $G_k^r(\hat{\mu})$, $H_k^r(\hat{\mu})$, defined by corresponding normalization conditions at the normalization point $\hat{\mu}$ ($k = 1, 2$):

$$\frac{1}{N}\frac{\partial^2 V}{\partial \bar{\sigma}_k^2}\bigg|_{\bar{\sigma}_k=\hat{\mu}} = \frac{1}{G_k(\Lambda)} - \frac{\Lambda}{\pi} + \frac{2\hat{\mu}}{\pi} \equiv \frac{1}{G_k^r(\hat{\mu})}, \tag{44}$$

$$\frac{1}{N}\frac{\partial^2 V}{\partial \bar{\varphi}_k^2}\bigg|_{\bar{\varphi}_k=\hat{\mu}} = \frac{1}{H_k(\Lambda)} - \frac{\Lambda}{\pi} + \frac{2\hat{\mu}}{\pi} \equiv \frac{1}{H_k^r(\hat{\mu})}. \tag{45}$$

Here $V \equiv \Omega_{\rm vac}^{\rm reg}(0,0)$ denotes the effective potential, and the second derivative in Eq. (44) has to be taken at $\bar{\sigma}_k = \hat{\mu}$, $\bar{\sigma}_j = 0$ ($j \neq k$), $\bar{\varphi}_k = 0$ etc.

Using Eqs. (44) and (45), one can consider new coupling-type parameters g_k, h_k:

$$\frac{1}{g_k} \equiv \frac{1}{G_k(\Lambda)} - \frac{\Lambda}{\pi} = \frac{1}{G_k^r(\hat{\mu})} - \frac{2\hat{\mu}}{\pi}, \tag{46}$$

$$\frac{1}{h_k} \equiv \frac{1}{H_k(\Lambda)} - \frac{\Lambda}{\pi} = \frac{1}{H_k^r(\hat{\mu})} - \frac{2\hat{\mu}}{\pi}. \tag{47}$$

Obviously, the bare coupling constants $G_k(\Lambda)$ and $H_k(\Lambda)$ (considered now as functions of Λ) are independent of the normalization point $\hat{\mu}$.

It thus follows from Eqs. (44)–(47) that the new coupling-type parameters g_k and h_k are also independent of $\hat{\mu}$ and, using analogous arguments, also independent of Λ. For brevity, the quantities g_k and h_k will be called coupling constants in what follows.

It is then possible to rewrite the expression (43) in the form of an ultraviolet-finite, renormalization-invariant quantity:

$$\Omega_{\rm vac}^{\rm ren}(0,0) = N\sum_{k=1}^{2}\left[\frac{1}{2g_k}\bar{\sigma}_k^2 + \frac{1}{2h_k}\bar{\varphi}_k^2 - \delta_{k1}\kappa\bar{\sigma}_1 + \frac{|M_k|^3}{6\pi}\right]. \tag{48}$$

Note that one gets attractive forces with $g_k < 0$, $h_k < 0$, if $G_k(\Lambda) > \pi/\Lambda$, $H_k(\Lambda) > \pi/\Lambda$ or, expressed in terms of renormalized quantities, for $G_k^r(\hat{\mu}) > \pi/(2\hat{\mu})$, $H_k^r(\hat{\mu}) > \pi/(2\hat{\mu})$.

It is instructive to compare this with results for the renormalization-group β functions, expressed in terms of rescaled dimensionless coupling constants $(\widetilde{G}_k^r, \widetilde{H}_k^r) \equiv (\hat{\mu}G_k^r, \hat{\mu}H_k^r)$.

Using Eqs. (46), (47), and $\partial g_k/\partial\hat{\mu} = \partial h_k/\partial\hat{\mu} = 0$, one obtains

$$\beta(\widetilde{G}_k^r) = \hat{\mu}\frac{\partial}{\partial\hat{\mu}}\widetilde{G}_k^r = \widetilde{G}_k^r\left(1 - \widetilde{G}_k^r/\widetilde{G}_k^{*r}\right), \tag{49}$$

$$\beta(\widetilde{H}_k^r) = \hat{\mu}\frac{\partial}{\partial\hat{\mu}}\widetilde{H}_k^r = \widetilde{H}_k^r\left(1 - \widetilde{H}_k^r/\widetilde{H}_k^{*r}\right), \tag{50}$$

where $\widetilde{G}_k^{*r} = \widetilde{H}_k^{*r} = \pi/2$.

Equations (49), (50) generalize the results for the usual GN model (see Ref. [18]) to the many-coupling case. In particular, we find that the quantities $G_k^{*r} = H_k^{*r} = \pi/(2\hat{\mu})$ correspond to nontrivial UV fixed points of the generalized, graphene-motivated GN model considered here.

Now, having demonstrated that the expression $\Omega_{\rm vac}^{\rm ren}(0,0)$ is UV-finite, it is clear that the condensate values $\bar{\sigma}_k(0,0)$, $\bar{\varphi}_k(0,0)$ at $T = \mu = 0$, following from the gap equations (31), (32), are described in terms of finite parameters g_k, h_k. Due to the explicit symmetry-breaking mass-like term κ in Eq. (48), the condensate $\bar{\sigma}_1$ depends not only on g_1, but also on κ.

Downloaded from https://academic.oup.com/ptep/article-abstract/2019/12/123I01/5651197 by Joint Institute for Nuclear Research user on 09 December 2019

Finally, it is worth remarking that in condensed-matter systems like graphene, the cutoff parameter Λ is an effective quantity, restricting the low-energy region of applicability of the considered model. In particular, $\Lambda = \mathcal{O}(1/a)$ is of the order of the inverse lattice spacing a.

For illustration, let us now consider the interesting case of an effective Coulomb interaction alone (compare discussions below Eq. (14)), where now $G_1' = G_2' = 1/4G^C \equiv G$ so that $g_k = h_k = g$. Moreover, supposing $G > \pi/\Lambda$, the renormalized coupling is attractive, $g < 0$. As shown in Appendix B, in this case we get $\bar{\sigma}_2 = \bar{\varphi}_k = 0$. The nonvanishing condensate $\bar{\sigma}_1$ satisfies the gap equation (B.9) and is given by

$$m \equiv \bar{\sigma}_1 = -\frac{\pi}{2g} \overset{+}{(-)} \sqrt{\left(\frac{\pi}{2g}\right)^2 + \pi\kappa} = M + \kappa|g| + \mathcal{O}(\kappa^2), \tag{51}$$

where we have introduced the mass-like term $M = \pi/|g|$. Note that the chosen positive solution realizes the total minimum of $\Omega_{\rm vac}$.

3.1.2. *Stationarity (gap) equations for $T \neq 0$, $\mu \neq 0$*

Using Eqs. (27), (28), (41), (48), one obtains the renormalized version of the thermodynamic potential

$$\Omega^{\rm ren}(T,\mu) = \Omega^{\rm ren}_{\rm vac} - \frac{N}{\beta}\sum_{k=1}^{2}\int \frac{d^2p}{(2\pi)^2}\left[\ln\left(1+e^{-\beta(E_p^{(k)}-\mu)}\right) + \ln\left(1+e^{-\beta(E_p^{(k)}+\mu)}\right)\right], \tag{52}$$

where the couplings g_k, h_k appearing in $\Omega^{\rm ren}_{\rm vac}$ are defined in Eqs. (46), (47). From Eqs. (31), (32), and (52) we obtain the following general expressions of stationarity (gap) equations ($\eta_k = \pm 1$ for $k = 1, 2$):

$$\frac{\bar{\sigma}_1}{\bar{\varrho}}\left\{\frac{\bar{\varrho}}{g_1} + \frac{(\bar{\sigma}_2+\bar{\varrho})^2}{2\pi} - \mathrm{sign}(\bar{\sigma}_2-\bar{\varrho})\frac{(\bar{\sigma}_2-\bar{\varrho})^2}{2\pi} + \right.$$
$$\left. + \sum_{k=1}^{2}\int \frac{d^2p}{(2\pi)^2}\eta_k\frac{M_k}{E_p^{(k)}}\left[f^+(E_p^{(k)}) + f^-(E_p^{(k)})\right]\right\} = \kappa, \tag{53}$$

$$\frac{\bar{\varphi}_i}{\bar{\varrho}}\left\{\frac{\bar{\varrho}}{h_i} + \frac{(\bar{\sigma}_2+\bar{\varrho})^2}{2\pi} - \mathrm{sign}(\bar{\sigma}_2-\bar{\varrho})\frac{(\bar{\sigma}_2-\bar{\varrho})^2}{2\pi} + \right.$$
$$\left. + \sum_{k=1}^{2}\int \frac{d^2p}{(2\pi)^2}\eta_k\frac{M_k}{E_p^{(k)}}\left[f^+(E_p^{(k)}) + f^-(E_p^{(k)})\right]\right\} = 0, \tag{54}$$

$$\left\{\frac{\bar{\sigma}_2}{g_2} + \frac{(\bar{\sigma}_2+\bar{\varrho})^2}{2\pi} - \mathrm{sign}(\bar{\sigma}_2-\bar{\varrho})\frac{(\bar{\sigma}_2-\bar{\varrho})^2}{2\pi} + \right.$$
$$\left. + \sum_{k=1}^{2}\int \frac{d^2p}{(2\pi)^2}\frac{M_k}{E_p^{(k)}}\left[f^+(E_p^{(k)}) + f^-(E_p^{(k)})\right]\right\} = 0. \tag{55}$$

Here $f^{\pm}(E)$ are Fermi–Dirac distribution functions,

$$f^{\pm}(E) = \frac{1}{e^{\beta(E\pm\mu)}+1}, \tag{56}$$

and $\mathrm{sign}(x)$ is the sign function.

For illustration, let us again consider the particular case of symmetric coupling constants $g_k = h_k \equiv g$, admitting, however, an explicit symmetry-breaking term $\kappa = m_0/G$ related to a finite bare

Downloaded from https://academic.oup.com/ptep/article-abstract/2019/12/123I01/5651197 by Joint Institute for Nuclear Research user on 09 December 2019

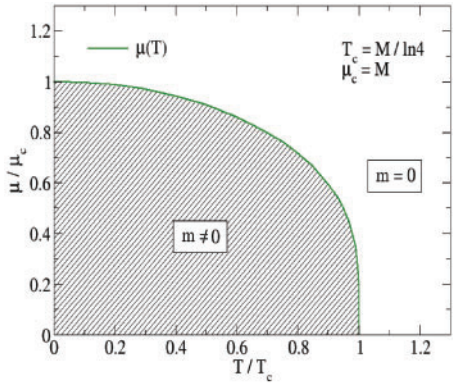

Fig. 1. Phase portrait for the GN model for $g < 0$, $\kappa = 0$ in the μ–T plane. The phases of no dynamical symmetry breaking ($m = 0$) and dynamical symmetry breaking ($m \neq 0$) are separated by a critical line $\mu(T)$ from Eqs. (61), (62).

fermion mass m_0. From Eqs. (53), (54) we then get $\bar{\varphi}_i = 0$, $\bar{\rho} = \bar{\sigma}_1$ in analogy to the vacuum case (cf. Appendix B). Let us consider in more detail the equations for the condensates $\bar{\sigma}_1$, $\bar{\sigma}_2$. By adding or subtracting Eqs. (53) and (55), one has ($M_{1,2} = \bar{\sigma}_2 \pm \bar{\sigma}_1$; $M = \pi/|g|$)

$$\frac{M_1}{\pi}\left\{-M + M_1 + 2\pi \int \frac{d^2p}{(2\pi)^2}\frac{1}{E_p^{(1)}}\left[f^+(E_p^{(1)}) + f^-(E_p^{(1)})\right]\right\} = \kappa, \tag{57}$$

$$\frac{(-M_2)}{\pi}\left\{-M + (-M_2) + 2\pi \int \frac{d^2p}{(2\pi)^2}\frac{1}{E_p^{(2)}}\left[f^+(E_p^{(2)}) + f^-(E_p^{(2)})\right]\right\} = \kappa\ ,\ (\bar{\sigma}_2 < \bar{\sigma}_1). \tag{58}$$

Comparing Eq. (58) with Eq. (57), one finds the solution $-M_2 = \bar{\sigma}_1 - \bar{\sigma}_2 = M_1 = \bar{\sigma}_1 + \bar{\sigma}_2$, $E_p^{(1)} = E_p^{(2)}$, and thus $\bar{\sigma}_2 = 0$, $M_{1,2} = \pm\bar{\sigma}_1$.

Finally, performing the momentum integral in Eq. (57) further gives

$$\frac{\bar{\sigma}_1}{\pi}\left\{-M + \bar{\sigma}_1 + \frac{1}{\beta}\ln\left[1 + 2e^{-\beta\bar{\sigma}_1}\cosh(\beta\mu) + e^{-2\beta\bar{\sigma}_1}\right]\right\} = \kappa. \tag{59}$$

Note that in the case of a small bare fermion mass m_0 (small κ), the system is characterized by a critical curve corresponding to a phase with a bare fermion mass and a phase with a larger dynamical mass $m = \bar{\sigma}_1$. In particular, by setting $\bar{\sigma}_1 = 0$, one obtains for the *chiral limit* $\kappa = 0$ from Eq. (59) an analytical expression for the critical line of a second-order phase transition, as sketched in the phase portrait of Fig. 1 (cf. Refs. [16,17]):

$$-M + \frac{1}{\beta}\ln\left[2 + 2\cosh(\beta\mu)\right] = 0. \tag{60}$$

As shown in Ref. [15], on the critical curve, the temperature and chemical potential are related by

$$\mu(T) = \frac{1}{\beta}\ln K(T), \tag{61}$$

$$K(T) = \left[-1 + \frac{1}{2}\exp(\beta M)\right] + \sqrt{\left[-1 + \frac{1}{2}\exp(\beta M)\right]^2 - 1}, \tag{62}$$

Downloaded from https://academic.oup.com/ptep/article-abstract/2019/12/123I01/5651197 by Joint Institute for Nuclear Research user on 09 December 2019

where in the chiral limit $M = \pi/|g|$ is the dynamical fermion mass m for the vacuum $T = \mu = 0$ (cf. Eq. (51)). Obviously, the function $\mu(T)$ in Eq. (61) vanishes for $K(T) = 1$ defining the critical temperature T_c,

$$-1 + \frac{1}{2}\exp(\beta_c M) = 1,\ T_c = M/(2\ln 2). \tag{63}$$

3.2. *Exciton fluctuations around mean fields*

Up to now we have treated the grand canonical partition function (24) in the mean-field (large-N saddle point) approximation. Let us now consider exciton fields as fields fluctuating around their mean-field values, restricting us to the case $\bar{\sigma}_1 \equiv \langle\sigma_1\rangle_{\rm mf} \neq 0$, $\bar{\sigma}_2 = \bar{\varphi}_1 = \bar{\varphi}_2 = 0$.[5] Then we have

$$\sigma_1(x) \longrightarrow \bar{\sigma}_1 + \sigma_1(x),\ \ \sigma_2(x) \longrightarrow \sigma_2(x),\ \ \varphi_{1,2}(x) \longrightarrow \varphi_{1,2}(x). \tag{64}$$

We can then decompose the inverse fermion propagator $S^{-1}(x,y)$ in Eq. (22) as

$$\begin{aligned} S^{-1}(x,y) &= (\gamma\partial - \mu\gamma_3 + m)\delta^{(3)}(x-y) + \Sigma(x)\delta^{(3)}(x-y) \\ &= S_{\rm mf}^{-1}(x-y) + \Sigma(x)\delta^{(3)}(x-y) \equiv S_{\rm mf}^{-1}\left[1 + S_{\rm mf}\Sigma\right], \end{aligned} \tag{65}$$

$$\Sigma(x) = \sigma_1(x) + \sigma_2(x)\gamma_{45} + \varphi_1(x)i\gamma_5 + \varphi_2(x)i\gamma_4, \tag{66}$$

where $m = \bar{\sigma}_1$. In the next step we will perform the path integration in Eq. (24) over fluctuating exciton fields in the Gaussian approximation (assuming again a suitable regularization of the vacuum term). For this aim, one has to expand the logarithm in the exponent up to the second (Gaussian) order in the fields

$$-N\left[\int d^3x\left(\frac{2\sigma_1\bar{\sigma}_1 + \sigma_1^2}{2G_1} - \kappa\sigma_1 + \frac{\sigma_2^2}{2G_2} + \frac{\varphi_1^2}{2H_1} + \frac{\varphi_2^2}{2H_2}\right) - {\rm Tr}S_{\rm mf}\Sigma + \frac{1}{2}{\rm Tr}\left(S_{\rm mf}\Sigma S_{\rm mf}\Sigma\right)\right]. \tag{67}$$

Obviously, the linear terms in the fluctuating fields in Eq. (67) vanish either due to the gap equation (31) or due to the corresponding vanishing of Tr $S_{\rm mf}[\Gamma_i]$ and Tr $S_{\rm mf}[\widetilde{\Gamma}_i]$. Performing then the field integration in the (bosonic) Gaussian integral

$$\mathcal{Z}_{\rm fl}(T,\mu) = \int\prod_{i=1}^{2}\mathcal{D}\sigma_i\mathcal{D}\varphi_i\exp\left\{-N\left[\int d^3x\sum_{k=1}^{2}\left(\frac{\sigma_k^2}{2G_k} + \frac{\varphi_k^2}{2H_k}\right) + \frac{1}{2}{\rm Tr}\left(S_{\rm mf}\Sigma S_{\rm mf}\Sigma\right)\right]\right\} \tag{68}$$

leads to the following factorizing contribution from exciton correlations corresponding to the σ_i and φ_i channels of interactions:

$$\mathcal{Z}_{\rm fl}(T,\mu) = \prod_{i=1,2}\left[\det\left(\beta\mathcal{D}_{\sigma_i}^{-1}\right)\right]^{-1/2}\cdot\left[\det\left(\beta\mathcal{D}_{\varphi_i}^{-1}\right)\right]^{-1/2}. \tag{69}$$

[5] In Refs. [20–22] additional excitonic corrections to the gap expression were considered. Such corrections were, however, shown to contribute in a higher order of $1/N$ and will thus be omitted here. The calculation of $\mathcal{O}(1/N)$ corrections from the composite excitons to the dynamical fermion mass and of $\mathcal{O}(1)$ corrections to the fermion polarization function can be straightforwardly done by using the variational path-integral approach of Ref. [46].

Downloaded from https://academic.oup.com/ptep/article-abstract/2019/12/123I01/5651197 by Joint Institute for Nuclear Research user on 09 December 2019

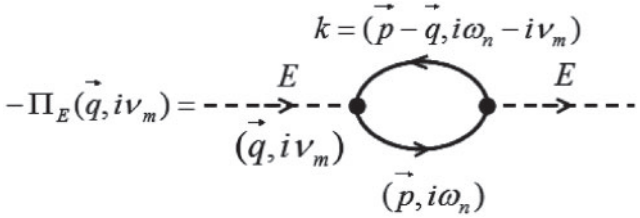

Fig. 2. Feynman diagram of the irreducible polarization function $\Pi_E(\vec{q},i\nu_m)$ for excitons $E=(\sigma_i,\varphi_i)$. The dots describe vertices Γ_E given by the Dirac matrices in Eq. (66), and the bold lines denote the mean-field fermion propagator $S_{\rm mf}(\vec{p},i\omega_n)$ of Eq. (71).

Here

$$\mathcal{D}_{\sigma_i}^{-1}=\frac{N}{G_i}-\Pi_{\sigma_i},\quad \mathcal{D}_{\varphi_i}^{-1}=\frac{N}{H_i}-\Pi_{\varphi_i} \tag{70}$$

are the inverse (bosonic) exciton propagators containing the polarization function Π_E of the exciton fields $E=(\sigma_i,\varphi_i)$, given by corresponding fermion loops, and suitable coordinate dependence is understood. The calculation of Eq. (70) is conveniently done by using Fourier transformation to momentum–frequency space $p=(\vec{p},\omega_n)$ and $q=(\vec{q},\nu_m)$ for the mean-field propagator $S_{\rm mf}(\vec{p},i\omega_n)$ and the polarization function $\Pi_E(\vec{q},i\nu_m)$, where $\omega_n=(2n+1)\pi/\beta$ and $\nu_m=2\pi m/\beta$ ($\{n,m\}=0,\pm1,\pm2,\ldots$) are the corresponding fermionic and bosonic Matsubara frequencies. Here the mean-field fermion propagator reads

$$S_{\rm mf}(\vec{p},i\omega_n)=(-\gamma_3(i\omega_n+\mu)-i\vec{\gamma}\cdot\vec{p}+m)^{-1}=\frac{\gamma_3(i\omega_n+\mu)+i\vec{\gamma}\cdot\vec{p}+m}{-(i\omega_n+\mu)^2+E_p^2}, \tag{71}$$

where

$$E_p=\sqrt{\vec{p}^2+m^2}, \tag{72}$$

and we now find it convenient to express the frequency dependence of the propagator by $i\omega_n$.

A straightforward, but lengthy calculation applying Matsubara summation techniques to loop diagrams of Fig. 2 (see Appendix C for details) leads to the following expression for the polarization function $\Pi_E(\vec{q},i\nu_m)$:

$$\Pi_E(\vec{q},i\nu_m)=-N\sum_{s,s'=\pm1}\int\frac{d^2p}{(2\pi)^2}\frac{f^-(s'E_k)-f^-(sE_p)}{i\nu_m+s'E_k-sE_p}\mathcal{T}^{\mp},$$
$$\mathcal{T}^{\mp}=1-ss'\frac{\vec{p}\cdot\vec{k}\mp m^2}{E_pE_k}. \tag{73}$$

Here the minus sign in $\mathcal{T}^{\mp}$ refers to the $\sigma_{1,2}$ excitons, whereas the plus sign refers to $\varphi_{1,2}$ and $f^{\pm}(E)$ are the Fermi–Dirac distribution functions introduced in Eq. (56). Obviously, the thermodynamic potential for exciton fluctuations follows then from the Fourier-transformed expression (69) to be given by

$$\Omega_{\rm fl}(T,\mu)=\frac{1}{2}\frac{1}{\beta l^2}\widetilde{\rm Tr}\left\{\sum_{i=1,2}\left[\ln\left(\beta\mathcal{D}_{\sigma_i}^{-1}(\vec{q},i\nu_m)\right)+\ln\left(\beta\mathcal{D}_{\varphi_i}^{-1}(\vec{q},i\nu_m)\right)\right]\right\}, \tag{74}$$

Downloaded from https://academic.oup.com/ptep/article-abstract/2019/12/123I01/5651197 by Joint Institute for Nuclear Research user on 09 December 2019

where the $\widetilde{\mathrm{Tr}}$ symbol refers to summation in $(\vec{q}, \nu_m)$ space. Consider now the total thermodynamic potential per flavor species:

$$\frac{1}{N}\Omega(T,\mu) = \frac{1}{N}\left(\Omega_{\rm mf} + \Omega_{\rm fl}\right). \tag{75}$$

Recalling that $\Omega_{\rm mf} = \mathcal{O}(N)$, the mean-field contribution in Eq. (75) is $\mathcal{O}(1)$, whereas the exciton fluctuating part $\Omega_{\rm fl}$ contributes in the large-N limit to (relative) order $\mathcal{O}(1/N)$, apart from an additive term $\mathcal{O}(\ln N/N)$ independent of m.

4. Equations for bound and resonant exciton states

4.1. Bound states

To study the corresponding equations for excitons in planar systems, we will closely follow here the analogous techniques of Refs. [31–33,41], used for studying $(3+1)$D models of colored quarks. The masses M_E of exciton bound states are determined by the poles of the exciton propagators or, equivalently, from the vanishing of the inverse propagators of excitons taken at rest, $\vec{q} = 0$,

$$\frac{N}{G_E} - \Pi_E(\vec{0}, i\nu_m = M_E) = 0, \tag{76}$$

where G_E are generic coupling constants ($G_E = \{G_{1,2}; H_{1,2}\}$), and the polarization function Π_E is analytically continued to real frequencies (energies) ω, $i\nu_m \to \omega = M_E + i\eta$. For $\vec{q} = 0$ one has $\vec{k} = \vec{p}$, and the only nonvanishing contribution in Eq. (73) emerges for $s \neq s'$ so that we can put $s' = -s$ and $ss' = -1$ in the following. The factor $\mathcal{T}^{\pm} \dashrightarrow \mathcal{T}^{\mp}$ then becomes

$$1 - ss'\frac{\vec{p}\vec{k} \mp m^2}{E_p E_k} = 1 + \frac{\vec{p}^2 \mp m^2}{E_p^2} = \begin{cases} 2\vec{p}^2/E_p^2 & \text{for } \Pi_{\sigma_{1,2}} \\ 2 & \text{for } \Pi_{\varphi_{1,2}} \end{cases}, \tag{77}$$

and the polarization function is equal to

$$\Pi_E(\vec{0}, M_E) = -2N \sum_s \int \frac{d^2p}{(2\pi)^2} \frac{f^-(-sE_p) - f^-(sE_p)}{M_E - s2E_p} \begin{pmatrix} p^2/E_p^2 \\ 1 \end{pmatrix}. \tag{78}$$

Using the relation

$$f^{\pm}\left(-E_p\right) = 1 - f^{\mp}\left(E_p\right), \tag{79}$$

performing the summation over the sign variable s and inserting the resulting expression into Eq. (76), one finally arrives at the (regularized) bound-state equation

$$\frac{N}{G_E} + 2N \int_\Lambda \frac{d^2p}{(2\pi)^2} \left[1 - f^+(E_p) - f^-(E_p)\right] \left(\frac{1}{M_E - 2E_p} - \frac{1}{M_E + 2E_p}\right) \begin{pmatrix} p^2/E_p^2 \\ 1 \end{pmatrix} = 0. \tag{80}$$

This equation determines the exciton masses M_E as functions of the coupling strength G_E, cutoff Λ, temperature T, chemical potential μ, and dynamical fermion mass $m(T,\mu)$. In general, it has to be solved numerically. However, it is also interesting to present its solution analytically in a closed form by using, for convenience, regularized integrals and bare coupling constants and postponing more detailed renormalization to a subsequent work devoted to the numerical analysis.

Downloaded from https://academic.oup.com/ptep/article-abstract/2019/12/123I01/5651197 by Joint Institute for Nuclear Research user on 09 December 2019

Let us start with the gap equation (31), which for the case $\bar{\sigma}_2 = \bar{\varphi}_i = 0$ takes the form

$$m(T,\mu) = \kappa G_1 + 2G_1 \int_\Lambda \frac{d^2p}{(2\pi)^2} \frac{m(T,\mu)}{E_p} \left[1 - f^+(E_p) - f^-(E_p)\right]. \tag{81}$$

Supposing a small bare fermion mass m_0 (small κ) and thus neglecting terms $\mathcal{O}(m_0^2)$, a straightforward calculation leads to the following mass spectra for the parity doublets (σ_1, φ_1), (σ_2, φ_2):

$$M^2_{\sigma_1}(T,\mu) = 4m^2(T,\mu) + \frac{\kappa}{m(T,\mu)} N g^2_{\sigma_1}(T,\mu), \tag{82}$$

$$M^2_{\varphi_1}(T,\mu) = \left[\frac{\kappa}{m(T,\mu)} + \left(\frac{1}{H_1} - \frac{1}{G_1}\right)\right] N g^2_{\varphi_1}(T,\mu), \tag{83}$$

$$M^2_{\sigma_2}(T,\mu) = 4m^2(T,\mu) + \left[\frac{\kappa}{m(T,\mu)} + \left(\frac{1}{G_2} - \frac{1}{G_1}\right)\right] N g^2_{\sigma_2}(T,\mu), \tag{84}$$

$$M^2_{\varphi_2}(T,\mu) = \left[\frac{\kappa}{m(T,\mu)} + \left(\frac{1}{H_2} - \frac{1}{G_1}\right)\right] N g^2_{\varphi_2}(T,\mu). \tag{85}$$

Here $g_E^2(T,\mu) = \left(\partial \Pi_E / \partial q^2|_{q^2=M_E^2}\right)^{-1}$ is the square of the induced fermion–exciton coupling constant appearing in the numerator of the exciton propagator in the pole approximation[6] (see, e.g., Eq. (30) of Ref. [46] for the case $T = \mu = 0$):

$$g_E^2(T,\mu) = \left\{ 2N \int_\Lambda \frac{d^2p}{(2\pi)^2} \frac{\left[1 - f^+(E_p) - f^-(E_p)\right]}{E_p \left(4E_p^2 - M_E^2\right)} \right\}^{-1}. \tag{86}$$

Note that g_E^2 behaves for large N as $g_E^2 = \mathcal{O}(1/N)$ so that the exciton masses in Eqs. (82)–(85) remain finite.

As expected, in the symmetric case of Coulomb-induced four-fermion interactions with $G_1 = G_2 = H_1 = H_2$, the masses of the (σ_1, σ_2) and (φ_1, φ_2) excitons are degenerate. In this case we have approximate continuous chiral symmetries of γ_5, γ_4 transformations, explicitly broken by the bare fermion mass term $m_0 \bar{\psi}\psi$. The φ_1, φ_2 excitons are then the would-be Goldstone bosons of the explicitly broken chiral symmetry.

As discussed in Sect. 2, there also exists the alternative case of a direct symmetry breaking in coupling constants. Indeed, the inclusion of a small on-site repulsive interaction term, arising in the case of a graphene lattice, as well as of phonon-mediated interactions, leads to an additional symmetry-breaking interaction, which altogether gives a modification of effective coupling constants with $G_1 = G_2 = G_1'$, $H_1 = H_2 = G_2'$, but $G_i \neq H_i$ (see Eqs. (14), (15)). In this case the masses of the doublets (σ_1, σ_2) and (φ_1, φ_2) remain (approximately) degenerate, but the (φ_1, φ_2) excitons no longer have typical masses of the order of $\mathcal{O}(\kappa)$ expected for standard would-be Goldstone bosons.

Finally, it is worth mentioning that there exists the important Mermin–Wagner–Coleman (MWC) no-go theorem [34,35], which for $(2+1)$D systems forbids spontaneous symmetry breaking (SSB) of a continuous symmetry for the case of finite temperature. Then, in the case of an exact chiral

[6] The expression for the exciton propagator contains the squared coupling constant g_E^2 and presents more precisely the T-matrix expression instead of a pure propagator. Nevertheless, for brevity, it is called a propagator here since both objects share the essential nonperturbative analytic property of the pole and branch cut structure in the complex plane.

Downloaded from https://academic.oup.com/ptep/article-abstract/2019/12/123I01/5651197 by Joint Institute for Nuclear Research user on 09 December 2019

symmetry with $\kappa = m_0 G_1 = 0$, this requires going beyond the leading $\mathcal{O}(1/N)$ exciton contributions (see Eq. (75)) obtained in the large-N expansion. In our case, this would require us to take into account phase fluctuations of exciton fields related to vortex excitations and the Kosterlitz–Thouless transition [16,17,47,48]. The consideration of corresponding higher-order $1/N$ corrections for the massless case $m_0 = 0$ is, however, beyond the scope of this paper. In this context, it is worth emphasizing that in the case of explicit symmetry breaking, as considered in this paper, there do not appear dangerous infrared singularities in loop diagrams due to the lack of massless particles. Therefore, the MWC theorem does not apply here (cf. discussions in Refs. [20–22]).

4.2. *Resonant exciton states*

Clearly, an exciton state becomes a resonant state if its mass exceeds two times the dynamical fermion mass so that it can decay into its constituent fermion–antifermion pair. In this case we are seeking a pole of the Fourier-transformed exciton propagators $\mathcal{D}_{\sigma_i}, \mathcal{D}_{\varphi_i}$, analytically continued into the second sheet of the complex frequency plane, $i\nu_n \to z = M_E - i\Gamma_E/2$.

Thus, we have to solve the equation

$$\frac{N}{G_E} - \Pi_E(\vec{0}, M_E - i\Gamma_E/2) = \\ = \frac{N}{G_E} - \left\{ 4NI_1 + 2N\left[(M_E - i\Gamma_E/2)^2 - \varepsilon_E^2\right] I_2(\vec{0}, M_E - i\Gamma_E/2) \right\} = 0, \tag{87}$$

where $\varepsilon_E = \{2m; 0\}$ for $E = \{\sigma_1(\sigma_2); \varphi_1(\varphi_2)\}$.

Here the two integrals I_1, I_2 are defined by

$$I_1 = \int_\Lambda \frac{d^2p}{(2\pi)^2} \frac{1}{2E_p} \left[1 - f^-(E_p) - f^+(E_p)\right], \tag{88}$$

$$I_2(\vec{0}, z) = \int_\Lambda \frac{d^2p}{(2\pi)^2} \frac{1}{4E_p^2} \left[1 - f^-(E_p) - f^+(E_p)\right] \left(\frac{1}{2E_p - z} + \frac{1}{2E_p + z}\right), \tag{89}$$

and $z = M_E - i\Gamma_E/2$.

Then, by separating Eq. (87) into one for the real part and another one for the imaginary part, one obtains

$$M_{E_i}^2 - \frac{1}{4}\Gamma_{E_i}^2 - \varepsilon_{E_i}^2 = \frac{\frac{1}{2G_{E_i}} - 2I_1}{|I_2(\vec{0}, M_{E_i})|^2} \mathrm{Re} I_2(\vec{0}, M_{E_i}), \tag{90}$$

$$M_{E_i}\Gamma_{E_i}^2 = \frac{\frac{1}{2G_{E_i}} - 2I_1}{|I_2(\vec{0}, M_{E_i})|^2} \mathrm{Im} I_2(\vec{0}, M_{E_i}). \tag{91}$$

The calculation of $\mathrm{Re}I_2$ and $\mathrm{Im}I_2$ appearing in Eqs. (90) and (91) can be done by using the standard formula

$$\frac{1}{x - x_0 \mp i\eta} = \mathrm{P.V.}\frac{1}{x - x_0} \pm i\pi\delta(x - x_0), \tag{92}$$

where P.V. means *principal value*.

After some lengthy but straightforward calculations, analogous to those in Ref. [49], one gets

$$\mathrm{Re} I_2 = \mathrm{P.V.} \int_\Lambda \frac{d^2p}{(2\pi)^2} \frac{1}{4E_p^2} \left[1 - f^-(E_p) - f^+(E_p)\right] \left(\frac{1}{2E_p - M_E} + \frac{1}{2E_p + M_E}\right), \tag{93}$$

Downloaded from https://academic.oup.com/ptep/article-abstract/2019/12/123I01/5651197 by Joint Institute for Nuclear Research user on 09 December 2019

$$\mathrm{Im}I_2 = \frac{1}{8M_E}\left[1 - f^-(\frac{M_E}{2}) - f^+(\frac{M_E}{2})\right]\Theta(M_E^2 - 4m^2)\Theta(4(\Lambda^2+m^2) - M_E^2), \tag{94}$$

where the UV cutoff Λ was used in performing the momentum integration and $\Theta(x)$ is the step function.

In deriving Eqs. (90) and (91) it was assumed that the imaginary part Γ_E occurring in the argument z of I_2 (which is the full width at half maximum of the Breit–Wigner distribution) is small compared to the mass M_E and may be neglected so that the equations for M_E and Γ_E decouple (compare with the discussions in Refs. [31,32]).

In the symmetric case $G_i = H_i$ one expects on general grounds that with increasing temperature the constituent fermion mass $m(T,\mu)$ and thus the two-particle threshold $2m(T,\mu)$ lowers, whereas the mass of the would-be Goldstone boson $M_{\varphi_1}(T,\mu)$ is chirally protected and thus rather temperature independent. Therefore it is inevitable that a temperature exists where the mass of φ_1 coincides with that of its constituents and thus the binding energy vanishes. This temperature is called *Mott temperature* T_{Mott} and is defined by the relation

$$M_{\varphi_1}(T_{\mathrm{Mott}},\mu) = 2m(T_{\mathrm{Mott}},\mu). \tag{95}$$

The effect of bound-state dissolution caused by a lowering of the continuum edge in a hot and dense medium is called the *Mott effect* due to its analogy with the physics of the insulator–metal transition according to Mott [50,51].

5. Beth–Uhlenbeck approach to the fermion–exciton plasma

Let us now investigate in more detail the thermodynamic potential $\Omega_{\mathrm{fl}}(T,\mu)$ for exciton fluctuations, given in Eq. (74), by rewriting the logarithm of the inverse exciton propagator as an integral:

$$\begin{aligned}\ln\left\{\beta\left[\frac{N}{G_E} - \Pi_E(\vec{q},i\nu_m)\right]\right\} &= \int_\varepsilon^1 d\lambda \frac{d}{d\lambda}\ln\left\{\beta\left[\frac{N}{\lambda G_E} - \Pi_E(\vec{q},i\nu_m)\right]\right\} + C \\ &= -\int_\varepsilon^1 \frac{d\lambda}{\lambda^2}\frac{N}{G_E}\frac{1}{\left[\frac{N}{\lambda G_E} - \Pi_E(\vec{q},i\nu_m)\right]} + C,\end{aligned} \tag{96}$$

considered in the limit $\varepsilon \to 0$, and $G_E = \{G_i, H_i\}, E = \{\sigma_i, \varphi_i\}$. Note that the frequency-independent constant $C = \ln[\beta N/(G_E\varepsilon)]$ compensates the logarithmic divergence of the integral at the lower boundary ε and reproduces the logarithmic dependence on N and β of the l.h.s. Next, it is convenient to rewrite the exciton propagator $\mathcal{D}_E^\lambda$ with coupling constant λG_E as a dispersion relation with the spectral function $A_E^\lambda(\vec{q},\omega)$ [52]:

$$-\int_\varepsilon^1 \frac{d\lambda}{\lambda^2}\frac{N}{G_E}\frac{1}{\left(\frac{N}{\lambda G_E} - \Pi_E(\vec{q},i\nu_m)\right)} - \ln\varepsilon = -\int_\varepsilon^1 \frac{d\lambda}{\lambda^2}\frac{N}{G_E}\int_{-\infty}^{\infty}\frac{d\omega}{2\pi}\frac{A_E^\lambda(\vec{q},\omega)}{\omega - i\nu_m}. \tag{97}$$

Recalling that the spectral function A_E^λ is given by the doubled imaginary part of the analytic continuation of the propagator to the real ω-axis at positions $\omega \pm i\eta$, where it has branch cuts, one obtains

$$\begin{aligned}\int_\varepsilon^1 \frac{d\lambda}{\lambda^2}\frac{N}{G_E}A_E^\lambda(\vec{q},\omega) &= -i\int_\varepsilon^1 \frac{dg}{\lambda^2}\frac{N}{G_E}\left[\mathcal{D}_E^\lambda(\vec{q},\omega+i\eta) - \mathcal{D}_E^\lambda(\vec{q},\omega-i\eta)\right] \\ &= -i\ln\frac{\frac{N}{G_E} - \Pi_E(\vec{q},\omega-i\eta)}{\frac{N}{G_E} - \Pi_E(\vec{q},\omega+i\eta)} = -i\ln\frac{\mathcal{D}_E(\vec{q},\omega+i\eta)}{\mathcal{D}_E(\vec{q},\omega-i\eta)}.\end{aligned} \tag{98}$$

Downloaded from https://academic.oup.com/ptep/article-abstract/2019/12/123I01/5651197 by Joint Institute for Nuclear Research user on 09 December 2019

It is worth remarking that the argument of the logarithm in the obtained expression is the very definition of the scattering matrix S_E in the Jost representation [31,32]:

$$S_E(\vec{q},\omega) = \frac{\mathcal{D}_E(\vec{q},\omega+i\eta)}{\mathcal{D}_E(\vec{q},\omega-i\eta)}. \tag{99}$$

Because above the threshold for elastic scattering $|S_E| = 1$, one has

$$S_E(\vec{q},\omega) = e^{2i\phi_E}, \tag{100}$$

where ϕ_E is the phase of $\mathcal{D}_E(\vec{q},\omega+i\eta)$. Then, using Eqs. (96)–(100), one gets

$$\ln\left(\beta\mathcal{D}_E^{-1}\right) = \int_{-\infty}^{\infty}\frac{d\omega}{\pi}\frac{1}{i\nu_m-\omega}\phi_E(\vec{q},\omega) + C', \tag{101}$$

where $C' = \ln(\beta N/G_E)$.

Finally, by inserting the expression (101) into the fluctuating part of the thermodynamic potential (74) and performing the trace over momenta and bosonic Matsubara frequencies ν_m (compare Eq. (C.11) in Appendix C), one obtains

$$\Omega_{\rm fl}(T,\mu) = -\sum_E\int\frac{d^2q}{(2\pi)^2}\int_{-\infty}^{\infty}\frac{d\omega}{2\pi}g(\omega)\phi_E(\vec{q},\omega), \tag{102}$$

where $g(\omega)$ denotes the Bose–Einstein distribution function

$$g(\omega) = [\exp(\beta\omega)-1]^{-1}, \tag{103}$$

and an additive term $\mathcal{O}(\ln N)$ independent of m is discarded (cf. the discussion below Eq. (75)).

It is convenient to split the integral (102) in the following way:

$$\begin{aligned}\Omega_{\rm fl}(T,\mu) &= -\sum_E\int\frac{d^2q}{(2\pi)^2}\left[\int_{-\infty}^{0}\frac{d\omega}{2\pi}g(\omega)\phi_E(\vec{q},\omega)+\int_0^{\infty}\frac{d\omega}{2\pi}g(\omega)\phi_E(\vec{q},\omega)\right]\\ &= -\sum_E\int\frac{d^2q}{(2\pi)^2}\int_0^{\infty}\frac{d\omega}{2\pi}\left[g(-\omega)\phi_E(\vec{q},-\omega)+g(\omega)\phi_E(\vec{q},\omega)\right].\end{aligned} \tag{104}$$

Next, by using the properties $\phi_E(\vec{q},-\omega)\equiv-\phi_E(\vec{q},\omega)$ and $g(-\omega) = -(1+g(\omega))$, and performing a partial integration, we obtain the final form of the excitonic thermodynamic potential:

$$\Omega_{\rm fl}(T,\mu) = \sum_E\int\frac{d^2q}{(2\pi)^2}\int_0^{\infty}\frac{d\omega}{2\pi}\left[\omega+\frac{2}{\beta}\ln\left(1-e^{-\beta\omega}\right)\right]\frac{d\phi_E}{d\omega}, \tag{105}$$

which is the so-called extended Beth–Uhlenbeck equation. The connection with the original Beth–Uhlenbeck expression for the second virial coefficient in terms of the two-body scattering phase shift can be found in Refs. [36,37]. Combining a possible pole term of the S matrix and the scattering contribution gives

$$\frac{d\phi_E(\vec{q},\omega)}{d\omega} \longrightarrow \pi\delta(\omega-E_E) + \left.\frac{d\phi_E(\vec{q},\omega)}{d\omega}\right|_{\rm scatt}. \tag{106}$$

Downloaded from https://academic.oup.com/ptep/article-abstract/2019/12/123I01/5651197 by Joint Institute for Nuclear Research user on 09 December 2019

Note that in the pole approximation only the first term in Eq. (106) is taken into account with $E_E = \sqrt{\vec{q}^2 + M_E^2}$. In this case one obtains from Eq. (105) the thermodynamic potential for a (quasi)relativistic Bose gas of non-interacting excitons:

$$\Omega_{\rm fl}^{\rm gas}(T,\mu) = \sum_E \int \frac{d^2q}{(2\pi)^2} \left[\frac{1}{2} E_E + \frac{1}{\beta} \ln\left(1 - e^{-\beta E_E}\right) \right]. \tag{107}$$

Correspondingly, the pressure of a gas of free excitons is given by

$$P_{\rm fl} = -\Omega_{\rm fl}^{\rm gas}(T,\mu) = -\sum_E \int \frac{d^2q}{(2\pi)^2} \left[\frac{1}{2} E_E + \frac{1}{\beta} \ln\left(1 - e^{-\beta E_E}\right) \right]. \tag{108}$$

Here the divergent momentum integral of the excitonic vacuum energy again has to be regularized by a cutoff and should be subtracted afterwards (see discussion below).

It is generally convenient to perform the variable transformation $\omega = \sqrt{\vec{q}^2 + s}$ in Eq. (105) and to introduce the density of states:

$$D_E(s) = \frac{1}{\pi} \frac{d\phi_E(s)}{ds}. \tag{109}$$

This leads to the alternative representation

$$\Omega_{\rm fl}(T,\mu) = \sum_E \int \frac{d^2q}{(2\pi)^2} \left\{ \int_{-\vec{q}^2}^{\infty} ds \left[\frac{1}{2}\sqrt{\vec{q}^2 + s} + \frac{1}{\beta} \ln\left(1 - e^{-\beta\sqrt{\vec{q}^2+s}}\right) \right] D_E(s) \right\}. \tag{110}$$

The total thermodynamic potential per flavor species is then given by Eqs. (75), (110).

As is well known, the equation of state and relevant thermodynamic relations are encoded in $\Omega(T,\mu; m(T,\mu))$, which corresponds to the pressure density up to a sign. Obviously, only the pressure density relative to the physical vacuum term $\Omega_{\rm vac}^{\rm phys}$ at $T = \mu = 0$

$$\Omega_{\rm vac}^{\rm phys} = \Omega_{\rm vac}^{\rm mf} + \Omega_{\rm fl}\Big|_{T=\mu=0} \tag{111}$$

can be measured. Here the mean-field vacuum expression $\Omega_{\rm vac}^{\rm mf}$ is given in Eq. (42) and the term $\Omega_{\rm fl}\Big|_{T=\mu=0}$ has to be taken from Eq. (110). Following an analogous procedure as for $(3+1)$D models of colored quarks in Refs. [31,32], the above vacuum term should be subtracted to give the physical thermodynamic potential

$$\widetilde{\Omega}(T,\mu) = \Omega(T,\mu) - \Omega_{\rm vac}^{\rm phys}, \tag{112}$$

which is again denoted by $\Omega(T,\mu)$. Clearly, such a removal of the divergent vacuum energy contributions leads to a vanishing pressure $P(T,\mu) = 0$ at $T = \mu = 0$. This procedure is analogous to the "no sea" approximation in relativistic mean-field approaches as, e.g., used in the Walecka model [33].

Finally, let us return to the expression given in Eq. (110) and consider the first departure beyond the pole approximation used in Eq. (107). Clearly, not too far above the Mott temperature $T_{\rm Mott}$ it is justified to describe $D_E(s)$ by a Breit–Wigner-type function (see a related proposal for quark matter in Ref. [33]):

$$D_E^R(s) = a_R \frac{M_E \Gamma_E}{(s - M_E^2)^2 + (M_E\Gamma_E)^2}. \tag{113}$$

Downloaded from https://academic.oup.com/ptep/article-abstract/2019/12/123I01/5651197 by Joint Institute for Nuclear Research user on 09 December 2019

Here M_E is the exciton pole mass, Γ_E is the corresponding width, and a_R is a normalization factor. Below $T_{\rm Mott}$, where the spectral broadening $\Gamma_E(T)$ of the state vanishes, the above expression becomes a delta function, typical for the spectral contribution of an exciton bound state (see Eq. (106)). The exciton phase shift ϕ_E^R corresponding to Eq. (113) should then be of the form [41]

$$\phi_E^R(s) = \frac{\pi}{\frac{\pi}{2} - \arctan\left(\frac{4m^2 - M_E^2}{M_E\Gamma_E}\right)} \left[\arctan\left(\frac{s - M_E^2}{M_E\Gamma_E}\right) - \arctan\left(\frac{4m^2 - M_E^2}{M_E\Gamma_E}\right)\right] \tag{114}$$

and represents, by construction, the resonant properties of excitonic correlations. As discussed in detail in the case of a $(3+1)$D Nambu–Jona-Lasinio quark model [31,32] and also applying here, the pole approximation alone is insufficient to fulfill Levinson's theorem [53]. In our case, it reads

$$\int_{4m^2}^{\infty} ds D_E(s) = 0. \tag{115}$$

Obviously, Eq. (115) requires that the density function must take both positive as well as negative values in such a way that the integral can vanish. As discussed for quark models [31,32,41,42], this should be the case, if a corresponding background scattering contribution $\phi_E^{\rm sc}$ is taken into account leading to the decomposition

$$\phi_E = \phi_E^{\rm R} + \phi_E^{\rm sc}. \tag{116}$$

We expect an analogous argumentation to apply to the generalized $(2+1)$D GN model considered here.

6. Summary and conclusions

In this paper we have extended the investigation of the generalized, graphene-motivated $(2+1)$D GN model of Ref. [29], performed at $T = 0$, to the case of finite temperature and fermion density (chemical potential) and have also gone beyond the mean-field approximation. The schematic model with four different types of four-fermion interactions considered here arises in a natural way by Fierz-transforming an effective electromagnetic Coulomb interaction onto four types of $f\bar{f}$-channels. The model includes further a small symmetry-breaking repulsive on-site interaction term and a small bare fermion mass that explicitly breaks chiral symmetry. The bare fermion mass term avoids IR-divergences and the validity of the MWC no-go theorem.

Throughout, we have used the powerful tool of large-N path-integral techniques to derive the bosonized version of the grand canonical partition function and the related thermodynamic potential in terms of four composite exciton fields $E = \{\sigma_i, \varphi_i\}$ $(i = 1, 2)$. We then first employ the large-N saddle point approximation to the path integral, which is based on the mean-field values $\{\bar{\sigma}_i, \bar{\varphi}_i\}$. They are determined from the minimum of the thermodynamic potential in the form of gap equations that are studied in some detail. The mean-field approximation just leads to the dominant contribution in the thermodynamic potential and the related equation of state. On the other hand, as is well known from four-quark models of strong interactions (see, e.g., Refs. [20–22,31–33]), light composite (would-be) Goldstone mesons (pions) play an important role in the low-temperature region of a quark–meson plasma, where quarks are heavy due to a nonvanishing quark condensate. At higher temperatures the dynamical quark mass decreases, the quark threshold lowers, and mesons are expected to become heavier resonances. Thus, in the high-temperature region fermions should dominate thermodynamics. As emphasized in the literature, it is just this different behavior in the low- and high-T regions that

Downloaded from https://academic.oup.com/ptep/article-abstract/2019/12/123I01/5651197 by Joint Institute for Nuclear Research user on 09 December 2019

makes it necessary to extend the large-N path-integral approach beyond the mean field by including contributions of fluctuating fields at (relative) order $\mathcal{O}(1/N)$ [20–22,31,32]. We followed here an analogous line of argumentation for the chosen graphene-motivated GN_3 model. In particular, we present the thermodynamic potential of the resulting fermion–exciton plasma at next order in the $1/N$ expansion. Besides general expressions for the fermion and exciton spectra at finite temperatures and densities, one of the main results is the presentation of the exciton contribution to the thermodynamic potential in a form that extends the results of Beth and Uhlenbeck [35] as well as Dashen et al. [37] to the in-medium case. The numerical calculation of the thermodynamic potential and the numerical estimate of the importance of the $\mathcal{O}(1/N)$ corrections within the underlying generalized GN_3 model are underway.

Acknowledgements

One of the authors (D.E.) thanks K. G. Klimenko and V. Ch. Zhukovsky for a long-term fruitful cooperation and many useful discussions. D.B. is grateful to N. T. Gevorgyan for assistance with preparing the manuscript. The authors acknowledge support by the DAAD partnership program between the Humboldt University Berlin and the University of Wroclaw and the hospitality extended to them at these institutions. D.B. was supported by the Polish Narodowe Centrum Nauki (NCN) under grant No. UMO-2014/15/B/ST2/03752 and by the RUDN University Program 5–100.

Appendix A. Dirac matrices in $D = 3$

A.1. Algebra

We find it convenient to use the reducible 4×4 chiral (Weyl) representation of Dirac matrices arising in a natural way in low-energy effective Lagrangians of hexagonal graphene-like lattice sheets (see, e.g., Refs. [29,44] and references therein). In Euclidean notation, where $\gamma_k^e = -i\gamma^k$, $k = 1, 2$, and $\gamma_3^e = \gamma^0$, we have Hermitian matrices (omitting now the index "e")

$$\gamma_k = \begin{pmatrix} 0 & i\tau_k \\ -i\tau_k & 0 \end{pmatrix}, \quad \gamma_3 = \begin{pmatrix} 0 & I_2 \\ I_2 & 0 \end{pmatrix} \quad (k = 1, 2), \tag{A.1}$$

with τ_k, I_2 being 2×2 Pauli matrices and the 2×2 unit matrix, respectively. In addition, there exist two "chiral" 4×4 matrices, which anticommute with all γ_μ ($\mu = 1, 2, 3$) and with each other,

$$\gamma_4 = \begin{pmatrix} 0 & i\tau_3 \\ -i\tau_3 & 0 \end{pmatrix}, \quad \gamma_5 = \gamma_1\gamma_2\gamma_3\gamma_4 = \begin{pmatrix} I_2 & 0 \\ 0 & -I_2 \end{pmatrix}, \tag{A.2}$$

as well as their combination:

$$\gamma_{45} = \frac{1}{2}[i\gamma_4, \gamma_5] = \begin{pmatrix} 0 & \tau_3 \\ \tau_3 & 0 \end{pmatrix}. \tag{A.3}$$

Note that γ_{45} commutes with all γ_μ, but anticommutes with γ_4 and γ_5. The matrices γ_μ ($\mu = 1, \ldots, 4$) satisfy the Euclideanized Dirac algebra

$$\{\gamma_\mu, \gamma_\nu\} = 2\delta_{\mu\nu} I, \tag{A.4}$$

where I is the 4×4 unit matrix. It is interesting to note that in the "chiral limit" $m_0 = 0$ ($\mu = 0$) the matrices (A.2)–(A.3) are the generators t_i,

$$t_1 = \frac{1}{2}\gamma_4, \quad t_2 = \frac{1}{2}\gamma_5, \quad t_3 = \frac{1}{2}\gamma_{45}, \tag{A.5}$$

Downloaded from https://academic.oup.com/ptep/article-abstract/2019/12/123I01/5651197 by Joint Institute for Nuclear Research user on 09 December 2019

of a symmetry group $SU(2)$ of the free Lagrangian $\mathcal{L}_0$ in Eq. (2) with group algebra

$$\left[t_i, t_j\right] = i\varepsilon_{ijk} t_k, \tag{A.6}$$

where ε_{ijk} is the Levi–Civita symbol.

A.2. Relations to graphene

For possible applications to planar systems in condensed-matter physics, it is worth comparing with corresponding notations used in the chiral limit ($m_0 = 0$) in graphene (see Refs. [29,44]; for an excellent review, see also Ref. [25] and references therein). As is well known, the above $SU(2)$ group describes there an emergent global continuous "pseudospin-valley" symmetry. Moreover, one considers chiral spinors $\psi_\pm = \frac{1}{2}(1 \pm \gamma_5)\psi$, which have chirality eigenvalues ± 1:

$$\gamma_5 \psi_\pm = \pm \psi_\pm. \tag{A.7}$$

They correspond to fermion excitations at the two inequivalent "Dirac points" $\vec{\mathrm{K}}_+, \vec{\mathrm{K}}_- = -\vec{\mathrm{K}}_+$ at the corners of the first Brillouin zone, where band energies vanish, $\varepsilon_\pm(\vec{\mathrm{K}}_\pm) = 0$. In particular, by performing a low-momentum expansion $\vec{k} = \vec{\mathrm{K}}_+(\vec{\mathrm{K}}_-) + \vec{p}$ around these points, one obtains a linear dispersion law $\varepsilon_\pm = \pm v_\mathrm{F}|\vec{p}|$ for massless quasiparticles on the hexagonal graphene lattice, enabling a quasirelativistic description by a Dirac Lagrangian. Definite chirality eigenvalues ± 1 coincide with the so-called valley index $\eta = \pm 1$, characterizing the Dirac points $\vec{\mathrm{K}}_+$ and $\vec{\mathrm{K}}_-$. Besides two "Dirac point (valley)" degrees of freedom, graphene electrons possess in addition two "sublattice" or "pseudospin" d.o.f. The latter ones are associated with the two existing triangular sublattices of carbon atoms in the hexagonal graphene lattice to which an electron belongs. By combining the corresponding two valley and pseudospin (sublattice) d.o.f. into a four-spinor, it is just possible to define chiral 4×4 matrices (A2) and to introduce various types of fermion interactions. Finally, these analogies then allow us to apply nonperturbative methods of relativistic QFT, extensively used for studying dynamical mass generation and phase transitions in quark models of strong interactions, to fermion theories with dependence on various types of symmetry-breaking scenarios.

A.3. Discrete symmetries

Let us next consider a convenient choice of discrete symmetry transformations $\mathcal{P}, \mathcal{T}, \mathcal{C}$ based on the condensed-matter roots of the graphene-motivated GN_3 model considered in the text. We shall here follow the definitions of Gusynin et al. [44], which have to be slightly modified when using Euclidean notations and Grassmann fields.

Consider (reducible) four-spinor fields of graphene with components referring to two inequivalent Dirac points $\vec{\mathrm{K}}_+, \vec{\mathrm{K}}_- = -\vec{\mathrm{K}}_+$ and triangular sublattices with A and B sites of a hexagonal honeycomb lattice given by[7]

$$\psi = \begin{pmatrix} \psi^{\mathrm{A}}_{\mathrm{K}_+} \\ \psi^{\mathrm{B}}_{\mathrm{K}_+} \\ \psi^{\mathrm{B}}_{\mathrm{K}_-} \\ \psi^{\mathrm{A}}_{\mathrm{K}_-} \end{pmatrix}, \ \bar{\psi} = \psi^\dagger \gamma_3 = \left(\psi^{\mathrm{B}*}_{\mathrm{K}_-}, \psi^{\mathrm{A}*}_{\mathrm{K}_-}, \psi^{\mathrm{A}*}_{\mathrm{K}_+}, \psi^{\mathrm{B}*}_{\mathrm{K}_+}\right). \tag{A.8}$$

[7] Note that Fig. 1 of Ref. [44] for the hexagonal graphene lattice and the Brillouin zone with corresponding Dirac points $\vec{\mathrm{K}}_\pm$ slightly differs from Fig. 1 of Ref. [29]. It is worth remarking that the Fourier-transformed Grassmann components $\psi^{A}_{K_+}$, $\psi^{A^*}_{K_+}$ etc. correspond to their one-particle annihilation or creation operators a_{K_+}, $a^\dagger_{K_+}$ etc.

Downloaded from https://academic.oup.com/ptep/article-abstract/2019/12/123I01/5651197 by Joint Institute for Nuclear Research user on 09 December 2019

(Note that the sublattices A, B were exchanged in components at the $\vec{\mathrm{K}}_-$ point in order to get a suitable four-spinor notation.) For shortness, we have omitted here the combined flavor index a including the considered number $\tilde{N}$ of hexagonal monolayers and the number 2 of physical spin degrees of freedom, i.e., $a \equiv (i,\sigma)$ with $i = 1,\ldots,\tilde{N}$ and $\sigma = (\uparrow,\downarrow)$ so that $a = 1,\ldots,N = 2\tilde{N}$. Moreover, "*" denotes here the operation of Grassmann involution.

A.3.1. Spatial inversion $\mathcal{P}$

By definition, $\mathcal{P}$ exchanges points $x = (\vec{x},x_3) \to \tilde{x} = (-\vec{x},x_3)$ and momenta $\vec{p} = i\frac{\partial}{\partial\vec{x}} \to -i\frac{\partial}{\partial\vec{x}} = -\vec{p}$. It is then clear that it exchanges A and B sites (sublattices) and Dirac points ($\vec{\mathrm{K}}_+$, $\vec{\mathrm{K}}_- = -\vec{\mathrm{K}}_+$), respectively. A convenient choice for the spinor transformation by spatial inversion is given by

$$\mathcal{P}: \quad \psi(x) \to \gamma_3\psi(\tilde{x})\,, \quad \bar{\psi}(x) = \psi^\dagger(x)\gamma_3 \to \psi^\dagger(\tilde{x})\,, \tag{A.9}$$

or, explicitly,

$$\psi(x) \to \begin{pmatrix} \psi^{\mathrm{B}}_{\mathrm{K}_-}(\tilde{x}) \\ \psi^{\mathrm{A}}_{\mathrm{K}_-}(\tilde{x}) \\ \psi^{\mathrm{A}}_{\mathrm{K}_+}(\tilde{x}) \\ \psi^{\mathrm{B}}_{\mathrm{K}_+}(\tilde{x}) \end{pmatrix}. \tag{A.10}$$

For further application, let us also recall the well known rule that Grassmann involution of a product of fields and a complex number c gives, e.g.,

$$\left(c\psi^{A*}_{K_+}\psi^{B}_{K_+}\right)^* = c^*\psi^{B*}_{K_+}\psi^{A}_{K_+} \ \text{ etc.},$$

with c^* being the complex conjugate of c.

It is then, e.g., straightforward to see that the current transforms as

$$\bar{\psi}\gamma_\mu\psi \to \bar{\psi}\widetilde{\gamma_\mu}\psi\,, \ \text{ with } \ \widetilde{\gamma_\mu} = (-\vec{\gamma},\gamma_3),$$

as shown in Table 1.

A.3.2. Time reversal $\mathcal{T}$

The antiunitary time reversal operation reverses momentum and spin, but not sublattices, and it interchanges $\vec{K}_\pm$ points [44]. Accordingly, in Euclidean notations we shall take

$$\mathcal{T}: \quad \psi(x) \to (i\sigma_2)i\gamma_1\gamma_5\psi(x)\,, \quad \bar{\psi}(x) \to -\bar{\psi}(x)i\gamma_1\gamma_5(i\sigma_2), \tag{A.11}$$

or, explicitly,

$$\psi(x) \to (i\sigma_2)\begin{pmatrix} \psi^{\mathrm{A}}_{\mathrm{K}_-}(x) \\ \psi^{\mathrm{B}}_{\mathrm{K}_-}(x) \\ \psi^{\mathrm{B}}_{\mathrm{K}_+}(x) \\ \psi^{\mathrm{A}}_{\mathrm{K}_+}(x) \end{pmatrix}. \tag{A.12}$$

Here σ_2 acts on the indices of physical spin contained in the suppressed flavor index a. It is then straightforward to see that the current transforms, e.g., as $\bar{\psi}\gamma_\mu\psi \to \bar{\psi}\gamma_\mu\psi$; see Table 1. Antiunitary

Downloaded from https://academic.oup.com/ptep/article-abstract/2019/12/123I01/5651197 by Joint Institute for Nuclear Research user on 09 December 2019

time reversal includes complex conjugation of c-numbers. Note that in Euclidean space $\mathcal{T}$ does not change the sign of the Euclidean time x_3. It also does not change the spatial components of the currents (see also Table 1 of Ref. [54]).

A.3.3. Charge conjugation $\mathcal{C}$

Charge conjugation exchanges particles and antiparticles (holes) leaving their spin and momentum unchanged. This leads to the requirement that under $\mathcal{C}$ the fermion current should transform as $\bar{\psi}\gamma_\mu\psi \to -\bar{\psi}\gamma_\mu\psi$ and the two Dirac points $\vec{K}_\pm$ should remain invariant. The action of $\mathcal{C}$ on the four-spinor can then be taken as

$$\mathcal{C}: \quad \psi \to i\gamma_1\bar{\psi}^t\,, \quad \bar{\psi} \to (-i\gamma_1\psi)^t\,. \tag{A.13}$$

One can see that $\mathcal{C}$ exchanges A and B sublattices. Indeed,

$$\psi \to \begin{pmatrix} -\psi^{\mathrm{B}^*}_{\mathrm{K}_+} \\ -\psi^{\mathrm{A}^*}_{\mathrm{K}_+} \\ \psi^{\mathrm{A}^*}_{\mathrm{K}_-} \\ \psi^{\mathrm{B}^*}_{\mathrm{K}_-} \end{pmatrix}. \tag{A.14}$$

Note that the charge conjugation matrix $C = i\gamma_1$ satisfies the relations

$$C = -C^{-1} = -C^\dagger = -C^t\,, \quad C^2 = -1\,, \quad C\gamma_\mu^t C^{-1} = -\gamma_\mu. \tag{A.15}$$

With the above definitions, it indeed follows that $\bar{\psi}\gamma_\mu\psi \to -\bar{\psi}\gamma_\mu\psi$, as quoted in Table 1.

Appendix B. Stationarity/gap equations (vacuum case)

From the vacuum contribution to the thermodynamic potential in Eq. (48) one obtains the following stationarity/gap equations for the case of symmetric coupling constants, $g_k = h_k = g$:

$$\frac{\bar{\sigma}_1}{\bar{\rho}}\left(\frac{1}{g}\bar{\rho} + \frac{(\bar{\sigma}_2+\bar{\rho})^2}{2\pi} - \mathrm{sign}(\bar{\sigma}_2-\bar{\rho})\frac{(\bar{\sigma}_2-\bar{\rho})^2}{2\pi}\right) = \kappa, \tag{B.1}$$

$$\frac{\bar{\varphi}_i}{\bar{\rho}}\left(\frac{1}{g}\bar{\rho} + \frac{(\bar{\sigma}_2+\bar{\rho})^2}{2\pi} - \mathrm{sign}(\bar{\sigma}_2-\bar{\rho})\frac{(\bar{\sigma}_2-\bar{\rho})^2}{2\pi}\right) = 0, \tag{B.2}$$

$$\left(\frac{1}{g}\bar{\sigma}_2 + \frac{(\bar{\sigma}_2+\bar{\rho})^2}{2\pi} + \mathrm{sign}(\bar{\sigma}_2-\bar{\rho})\frac{(\bar{\sigma}_2-\bar{\rho})^2}{2\pi}\right) = 0. \tag{B.3}$$

Clearly, for a nonvanishing condensate $\bar{\varphi}_i \neq 0\,(i = 1, 2)$, the bracket in Eq. (B.2) should vanish, which for $\kappa \neq 0$ is, however, impossible due to Eq. (B.1). Thus, $\bar{\varphi}_i = 0$ and $\bar{\rho} = \sqrt{\bar{\sigma}_1^2 + \bar{\varphi}_1^2 + \bar{\varphi}_2^2} = |\bar{\sigma}_1|$. Analogously, $\bar{\sigma}_1 = \bar{\sigma}_2$ cannot be a solution of Eqs. (B.1), (B.3). It is convenient to rewrite Eq. (B.1) as $(\bar{\sigma}_1 > 0)$

$$\frac{1}{g}\bar{\sigma}_1 + \frac{\bar{\sigma}_1^2 + \bar{\sigma}_2^2}{\pi} = \kappa, \quad (\bar{\sigma}_2 < \bar{\sigma}_1), \tag{B.4}$$

$$\frac{1}{g}\bar{\sigma}_1 + \frac{2\bar{\sigma}_1\bar{\sigma}_2}{\pi} = \kappa, \quad (\bar{\sigma}_2 > \bar{\sigma}_1), \tag{B.5}$$

Downloaded from https://academic.oup.com/ptep/article-abstract/2019/12/123I01/5651197 by Joint Institute for Nuclear Research user on 09 December 2019

and, analogously, for Eq. (B.3),

$$\frac{1}{g}\bar{\sigma}_2 + \frac{\bar{\sigma}_1^2 + \bar{\sigma}_2^2}{\pi} = 0 \quad (\bar{\sigma}_2 > \bar{\sigma}_1), \tag{B.6}$$

$$\frac{1}{g}\bar{\sigma}_2 + \frac{2\bar{\sigma}_1\bar{\sigma}_2}{\pi} = 0 \quad (\bar{\sigma}_2 < \bar{\sigma}_1). \tag{B.7}$$

Since $\Omega_{\rm vac}^{\rm ren}$ in Eq. (48) is an even function of $\bar{\sigma}_2$, it is sufficient to study the global minimum of $\Omega_{\rm vac}^{\rm ren}$ and the resulting gap equations only on the set $\bar{\sigma}_{1,2} \geq 0$. Next, suppose $\bar{\sigma}_2 \neq 0$. In this case, one obtains $\bar{\sigma}_1 = -\frac{\pi}{2g}$ for $0 < \bar{\sigma}_2 < \bar{\sigma}_1$ from Eq. (B.7). Inserting this into Eq. (B.4) leads to

$$-\frac{\pi}{2g^2} + \frac{\pi}{4g^2} + \frac{\bar{\sigma}_2^2}{\pi} = \kappa\ , \quad \bar{\sigma}_2 = \sqrt{\frac{\pi^2}{4g^2} + \pi\kappa} > \bar{\sigma}_1, \tag{B.8}$$

which is in contradiction to our assumptions $\bar{\sigma}_2 \neq 0$ and $0 < \bar{\sigma}_2 < \bar{\sigma}_1$. Thus, the solutions of the vacuum gap equations (B.1)–(B.3) are $\bar{\varphi}_i = 0$, $\bar{\sigma}_2 = 0$, and a finite $\bar{\sigma}_1$, given by

$$\frac{1}{g}\bar{\sigma}_1 + \frac{\bar{\sigma}_1^2}{\pi} = \kappa, \ \ \bar{\sigma}_1 = -\frac{\pi}{2g}\ \overset{+}{(-)}\ \sqrt{\left(\frac{\pi}{2g}\right)^2 + \pi\kappa} = \mathrm{M} + \kappa|g| + O(\kappa^2). \tag{B.9}$$

Here we have introduced the mass term $\mathrm{M} = \pi/|g|$, which, in the chiral limit $\kappa = 0$, determines the dynamical fermion mass $\bar{\sigma}_1 \equiv m(T = 0, \mu = 0)$ at vanishing temperature and chemical potential. One can see that the chosen positive solution in Eq. (B.9) realizes the absolute minimum of $\Omega_{\rm vac}^{\rm ren}$.

Appendix C. Exciton polarization functions

It is straightforward to show that in momentum–frequency space the polarization function $\Pi_E(\bar{q}, i\nu_m)$ for excitons $E = \{\sigma_i; \varphi_i\}$, shown in Fig. 2, is given by

$$\Pi_E(\bar{q}, i\nu_m) = -4\frac{N}{\beta}\sum_n \int \frac{d^2p}{(2\pi)^2} \frac{(i\omega_n + \mu)(i\omega_n + \mu - i\nu_m) - \vec{p}\cdot\vec{k} \pm m^2}{\left[(i\omega_n + \mu)^2 - E_p^2\right]\left[(i\omega_n + \mu - i\nu_m)^2 - E_k^2\right]}, \tag{C.1}$$

where $\nu_m = 2\pi m/\beta$ are bosonic Matsubara frequencies, and the plus/minus sign in front of m^2 refers to $\sigma_{1,2}/\varphi_{1,2}$ excitons.

For pedagogical reasons and a better understanding of the important expression (73), we will now illustrate the detailed calculation of the polarization function (C.1), following the analogous procedure of Ref. [49], which was applied to (3 + 1)D models of quarks and composite mesons. First, in order to perform the fermionic Matsubara sum over n in expression (C.1), one uses standard partial fraction decompositions and a compact notation with a sign variable $s = \pm 1$ (a technique already used in Ref. [55]). A typical expression reads

$$\frac{1}{p_0^2 - E_j^2} = \frac{1}{2E_j}\left(\frac{1}{p_0 - E_j} - \frac{1}{p_0 + E_j}\right) = \sum_{s=\pm 1}\frac{1}{2E_j}\frac{s}{p_0 - sE_j}. \tag{C.2}$$

Substituting $p_0 \to i\omega_n + \mu - i\nu_m$ and using $s^2 = 1$, one gets

$$\sum_{s=\pm 1}\frac{1}{2E_j}\frac{s}{i\omega_n + \mu - i\nu_m - sE_j} = \sum_{s=\pm 1}\frac{1}{2E_j}\frac{s}{i\omega_n - i\nu_m - s(E_j - s\mu)}. \tag{C.3}$$

Downloaded from https://academic.oup.com/ptep/article-abstract/2019/12/123I01/5651197 by Joint Institute for Nuclear Research user on 09 December 2019

With this compact notation, the polarization function (C.1) is now written as

$$\Pi_E(\vec{q},i\nu_m) = -4\frac{N}{\beta}\sum_n \int \frac{d^2p}{(2\pi)^2}\sum_{s,s'}\frac{ss'}{4E_pE_k}\frac{(i\omega_n+\mu)(i\omega_n+\mu-i\nu_m)-\vec{p}\cdot\vec{k}\pm m^2}{\left(i\omega_n - s\xi_p^{(-s)}\right)\left(i\omega_n - i\nu_m - s'\xi_k^{(-s')}\right)}, \tag{C.4}$$

where

$$\xi_j^{(-s)} = E_j - s\mu. \tag{C.5}$$

Generally, the Matsubara sum over fermion frequencies is performed by using the standard formulae [56]:

$$\frac{1}{\beta}\sum_n \frac{1}{i\omega_n - x} = f(x) = \left(e^{\beta x}+1\right)^{-1}, \tag{C.6}$$

$$\frac{1}{\beta}\sum_n \frac{1}{(i\omega_n - sE)}\cdot\frac{1}{(i\omega_n - i\nu_m - s'E')} = \frac{f(s'E')-f(sE)}{i\nu_m + s'E' - sE}. \tag{C.7}$$

Here Eq. (C.7) simply follows by partial fraction decomposition and then application of Eq. (C.6). Note that the summation formula (C.7) cannot yet be directly applied to Eq. (C.4), since the numerator depends on ω_n. To get rid of this, it is convenient to rewrite the corresponding factors in the numerator by subtracting and adding suitable terms. One thus has

$$\begin{aligned}
&\frac{\left[\left(i\omega_n - s\xi_p^{(-s)}\right)+\left(s\xi_p^{(-s)}+\mu\right)\right]\left[\left(i\omega_n - i\nu_m - s'\xi_k^{(-s')}\right)+\left(s'\xi_k^{(-s')}+\mu\right)\right]}{\left(i\omega_n - s\xi_p^{(-s)}\right)\left(i\omega_n - i\nu_m - s'\xi_k^{(-s')}\right)}\\
&= \left(1+\frac{s\xi_p^{(-s)}+\mu}{i\omega_n - s\xi_p^{(-s)}}\right)\left(1+\frac{s'\xi_k^{(-s')}+\mu}{i\omega_n - i\nu_m - s'\xi_k^{(-s')}}\right)\\
&= \left[1+\frac{s\xi_p^{(-s)}+\mu}{i\omega_n - s\xi_p^{(-s)}}+\frac{s'\xi_k^{(-s')}+\mu}{i\omega_n - i\nu_m - s'\xi_k^{(-s')}}\right]+\frac{\left(s\xi_p^{(-s)}+\mu\right)\left(s'\xi_k^{(-s')}+\mu\right)}{\left(i\omega_n - s\xi_p^{(-s)}\right)\left(i\omega_n - i\nu_m - s'\xi_k^{(-s')}\right)}.
\end{aligned} \tag{C.8}$$

Using Eqs. (C.4), (C.6), and (C.8), one can see that the contribution of the square bracket term in the last line of Eq. (C.8) vanishes. Moreover, rewriting the factors in the numerator of the second term as $(s\xi_p^{(-s)}+\mu) = s(E_p - s\mu)+\mu = sE_p$ etc. gives

$$\Pi_E(\vec{q},i\nu_m) = -4\frac{N}{\beta}\sum_n \int \frac{d^2p}{(2\pi)^2}\sum_{s,s'}\frac{ss'}{4E_pE_k}\frac{sE_ps'E_k - \vec{p}\cdot\vec{k}\pm m^2}{\left(i\omega_n - s\xi_p^{(-s)}\right)\left(i\omega_n - i\nu_m - s'\xi_k^{(-s')}\right)}. \tag{C.9}$$

Finally, by now applying Eq. (C.7) and taking into account that $f(s'\xi_k^{(-s')}) = f(s'E_k-\mu) \equiv f^-(s'E_k)$ etc., one obtains

$$\begin{aligned}
\Pi_E(\vec{q},i\nu_m) &= -N\sum_{s,s'}\int\frac{d^2p}{(2\pi)^2}\frac{f^-(s'E_k)-f^-(sE_p)}{i\nu_m + s'E_k - sE_p}\mathcal{T}^{\mp},\\
\mathcal{T}^{\mp} &= 1 - ss'\frac{\vec{p}\cdot\vec{k}\mp m^2}{E_pE_k},
\end{aligned} \tag{C.10}$$

Downloaded from https://academic.oup.com/ptep/article-abstract/2019/12/123I01/5651197 by Joint Institute for Nuclear Research user on 09 December 2019

which is just the expression used in Eq. (73) of the main text. Note that in deriving Eq. (C.10) use has been made of the fact that for bosonic Matsubara frequencies $\nu_m = 2\pi m/\beta, f(x+\nu_m) = f(x)$. Let us remark that the compact notation of the excitonic polarization function (C.10) reproduces the general structure of the corresponding meson expression (3.9) of Hüfner et al. in Refs. [31,32].

For completeness, we also quote the Matsubara sum formula for bosons [56]:

$$\frac{1}{\beta}\sum_m \frac{1}{i\nu_m - x} = -g(x) = -\frac{1}{e^{\beta x}-1}. \tag{C.11}$$

Here $g(x)$ is the Bose–Einstein distribution, and ν_m are the bosonic Matsubara frequencies.

References

[1] J. Bardeen, L. N. Cooper, and J. R. Schrieffer, Phys. Rev. **108**, 1175 (1957).
[2] N. N. Bogoliubov, Sov. Phys. JETP **7**, 41 (1958) [Zh. Eksp. Teor. Fiz. **34**, 58 (1958)].
[3] Y. Nambu and G. Jona-Lasinio, Phys. Rev. **122**, 345 (1961).
[4] Y. Nambu and G. Jona-Lasinio, Phys. Rev. **124**, 246 (1961).
[5] T. Eguchi, Phys. Rev. D **14**, 2755 (1976).
[6] M. K. Volkov and D. Ebert, Sov. J. Nucl. Phys. **36**, 736 (1982) [Yad. Fiz. **36**, 1265 (1982)].
[7] D. Ebert and M. K. Volkov, Z. Phys. C **16**, 205 (1983).
[8] M. K. Volkov, Annals Phys. **157**, 282 (1984).
[9] D. Ebert and H. Reinhardt, Nucl. Phys. B **271**, 188 (1986).
[10] D. Ebert, H. Reinhardt, and M. K. Volkov, Prog. Part. Nucl. Phys. **33**, 1 (1994).
[11] D. J. Gross and A. Neveu, Phys. Rev. D **10**, 3235 (1974).
[12] D. J. Gross, in *Methods in Field Theory*, eds. R. Balian and J. Zinn-Justin (North-Holland, Amsterdam, 1976).
[13] K. G. Klimenko, Z. Phys. C **37**, 457 (1988).
[14] K. G. Klimenko, Z. Phys. C **54**, 323 (1992).
[15] A. S. Vshivtsev, B. V. Magnitsky, V. C. Zhukovsky, and K. G. Klimenko, Phys. Part. Nucl. **29**, 523 (1998) [Fiz. Elem. Chast. Atom. Yadra **29**, 1259 (1998)].
[16] B. Rosenstein, B. J. Warr, and S. H. Park, Phys. Rept. **205**, 59 (1991).
[17] B. Rosenstein, B. J. Warr, and S. H. Park, Phys. Rev. D **39**, 3088 (1989).
[18] H.-J. He, Y.-P. Kuang, Q. Wang, and Y.-P. Yi, Phys. Rev. D **45**, 4610 (1992).
[19] A. Okopińska, Phys. Rev. D **38**, 2507 (1988).
[20] A. Barducci, R. Casalbuoni, M. Modugno, G. Pettini, and R. Gatto, Mod. Phys. Lett. A **11**, 1579 (1996).
[21] M. Modugno, G. Pettini, and R. Gatto, Phys. Rev. D **57**, 4995 (1998).
[22] M. Modugno, Riv. Nuovo Cimento **23N5**, 1 (2000).
[23] A. J. Heeger, S. Kivelson, J. R. Schrieffer, and W.-P. Su, Rev. Mod. Phys. **60**, 781 (1988).
[24] D. K. Campbell and A. R. Bishop, Nucl. Phys. B **200**, 297 (1982).
[25] A. H. Castro Neto, F. Guinea, N. M. R. Peres, K. S. Novoselov, and A. K. Geim, Rev. Mod. Phys. **81**, 109 (2009).
[26] D. Ebert and V. N. Pervushin, Proc. XVIII Int. Conf. High Energy Physics, Vol. I, p. C125 (1976).
[27] D. Ebert and V. N. Pervushin, JINR preprint "Dynamical breakdown of chiral symmetry and abnormal perturbation expansions", E-10020, Dubna, 1976 (unpublished).
[28] H. Kleinert, Phys. Lett. B **62**, 429 (1976).
[29] D. Ebert, K. G. Klimenko, P. B. Kolmakov, and V. Ch. Zhukovsky, Annals Phys. **371**, 254 (2016).
[30] E. V. Gorbar, V. P. Gusynin, and V. A. Miransky, Phys. Rev. D **64**, 105028 (2001).
[31] J. Hüfner, S. P. Klevansky, P. Zhuang, and H. Voss, Annals Phys. **234**, 225 (1994).
[32] P. Zhuang, J. Hüfner, and S. P. Klevansky, Nucl. Phys. A **576**, 525 (1994).
[33] D. Blaschke, M. Buballa, A. Dubinin, G. Röpke, and D. Zablocki, Annals Phys. **348**, 228 (2014).
[34] N. D. Mermin and H. Wagner, Phys. Rev. Lett. **17**, 1133 (1966); **17**, 1307 (1966) [erratum].
[35] S. Coleman, Commun. Math. Phys. **31**, 259 (1973).
[36] E. Beth and G. E. Uhlenbeck, Physica **4**, 915 (1937).
[37] R. Dashen, S.-K. Ma, and H. J. Bernstein, Phys. Rev. **187**, 345 (1969); **6**, 851 (1972) [erratum].
[38] W. Ebeling, Ann. Phys. (Lpz.) **22**, 33 (1968).

Downloaded from https://academic.oup.com/ptep/article-abstract/2019/12/123I01/5651197 by Joint Institute for Nuclear Research user on 09 December 2019

[39] R. Zimmermann, *Many-Particle Theory of Highly Excited Semiconductors* (Teubner, Leipzig, 1987).
[40] M. Schmidt, G. Röpke, and H. Schulz, Annals Phys. **202**, 57 (1990).
[41] A. Wergieluk, D. Blaschke, Yu. L. Kalinovsky, and A. V. Friesen, Phys. Part. Nucl. Lett. **10**, 660 (2013).
[42] D. Blaschke, A. Dubinin, D. Ebert, and A. V. Friesen, Phys. Part. Nucl. Lett. **15**, 230 (2018).
[43] T. W. Appelquist, M. Bowick, D. Karabali, and L. C. R. Wijewardhana, Phys. Rev. D **33**, 3704 (1986).
[44] V. P. Gusynin, S. G. Sharapov, and J. P. Carbotte, Int. J. Mod. Phys. B **21**, 4611 (2007).
[45] J. I. Kapusta, *Finite Temperature Field Theory* (Cambridge University Press, Cambridge, UK, 1989).
[46] D. Blaschke and D. Ebert, Nucl. Phys. B **921**, 753 (2017).
[47] V. L. Berezinsky, Sov. Phys. JETP **32**, 493 (1971) [Zh. Eksp. Teor. Fiz. **59**, 907 (1971)].
[48] J. M. Kosterlitz and D. J. Thouless, J. Phys. C: Solid State Phys. **6**, 1181 (1973).
[49] A. Wergieluk, Generalized Beth-Uhlenbeck approach to a quark-meson plasma in the PNJL model. Master Thesis. University of Wroclaw, 2014.
[50] N. F. Mott, Rev. Mod. Phys. **40**, 677 (1968).
[51] R. Redmer, F. Hensel, and B. Holst (eds.), *Metal-to-Nonmetal Transitions* (Springer, Berlin, 2010), Springer Series in Materials Science, Vol. 132.
[52] H. Abuki, Nucl. Phys. A **791**, 117 (2007).
[53] N. Levinson, Mat.-Fys. Medd. **25**, 1 (1949).
[54] D. Mesterházy, J. Berges, and L. von Smekal, Phys. Rev. B **86**, 245431 (2012).
[55] M. Bellac, *Thermal Field Theory* (Cambridge University Press, Cambridge, UK, 2000).
[56] T. Matsubara, Prog. Theor. Phys. **14**, 351 (1955).

Downloaded from https://academic.oup.com/ptep/article-abstract/2019/12/123I01/5651197 by Joint Institute for Nuclear Research user on 09 December 2019